CMS Detector Upgrades for the HL-LHC

JULIE HOGAN, CMS COLLABORATION
BETHEL UNIVERSITY
APRIL 16, 2020

CMS HL-LHC Upgrades

- Huge fluences expected with HL-LHC luminosity (5.0-7.5 x 10^{34} / cm^2)
- Expect ~3000/fb over the course of the HL-LHC – upgraded detectors have to last and reconstruct physics objects well in 200 interaction conditions
- Rebuilds or extensions coming to most CMS subdetectors
- **CMS Phase-2 forward detectors could form a forward spectrometer**

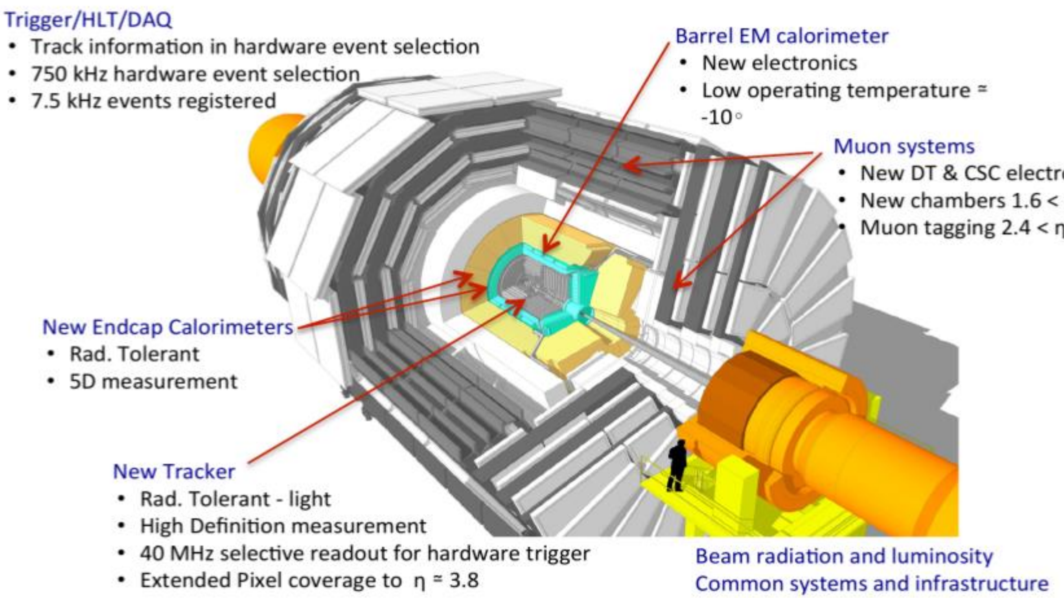

LHC: New low-b triplet quadropoles + crab cavities

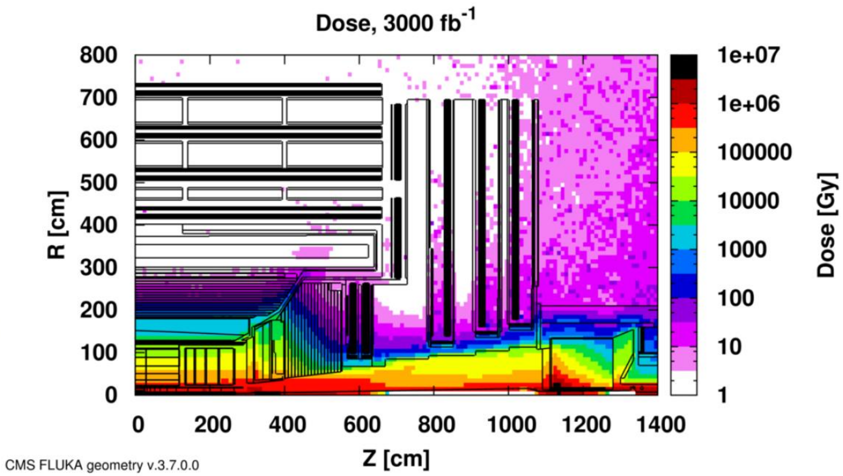

CMS Phase-2 for FMS?

- Silicon tracking, pixel-based
- Silicon timing layer, LGAD technology
- Silicon-based calorimetry
- Gas electron multiplier (+others) for muons
- **FMS: small-area versions around beampipe?**
  - ~0.25 m^2 annulus

M. Albrow

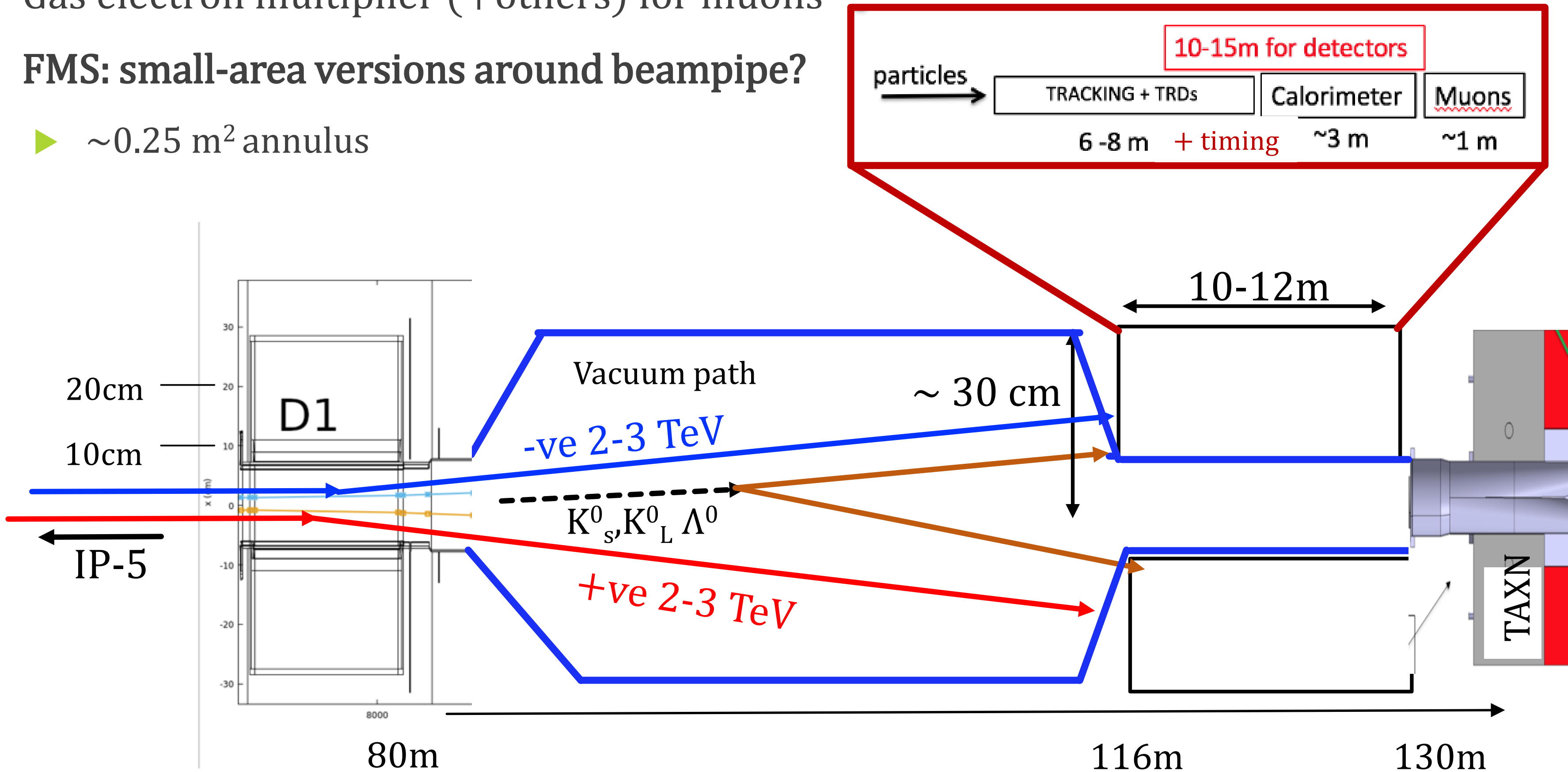

Tracking Upgrades

- Radiation tolerance: **blue = dead @ 1000/fb**
- Higher granularity for lower occupancy
- Increased coverage, pixels out to |η| ~ 4
- Whole tracker will use two-phase CO_2 cooling

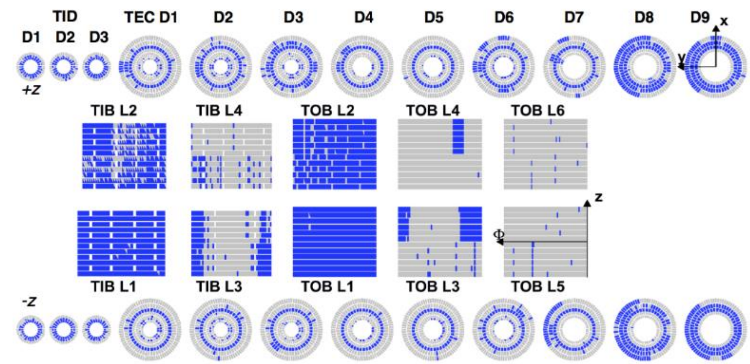

CMS TP

Trk TDR

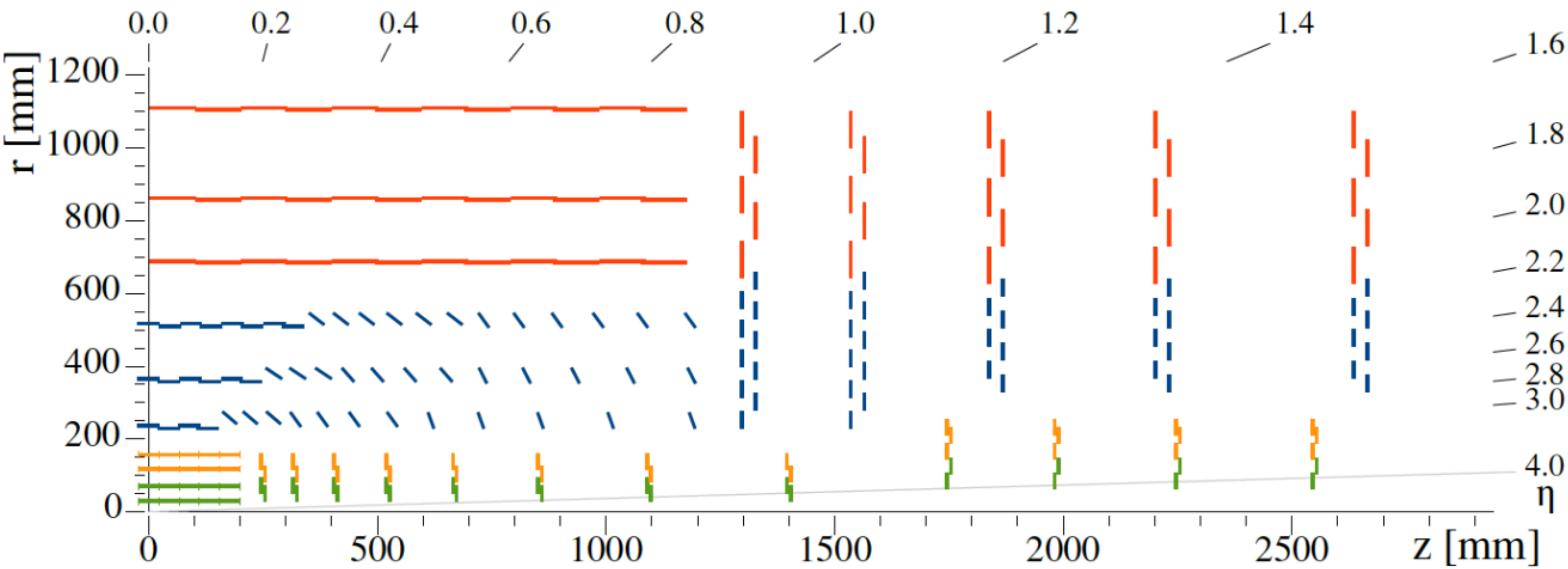

Tracking Upgrades

- Inner tracker: n-in-p pixels of 25 x 100 μm
- Outer tracker: n-in-p sensors with 100 μm strips or 100x1400 μm macro-pixels
- Pairs of sensors in each module, modules in layers overlap in z and ϕ

IT:

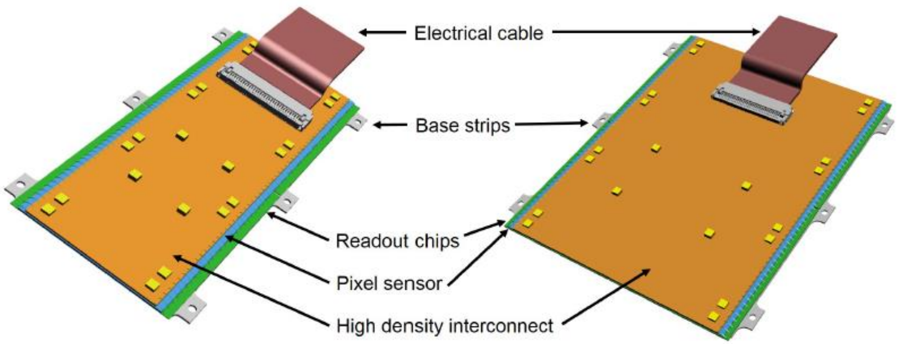

OT:

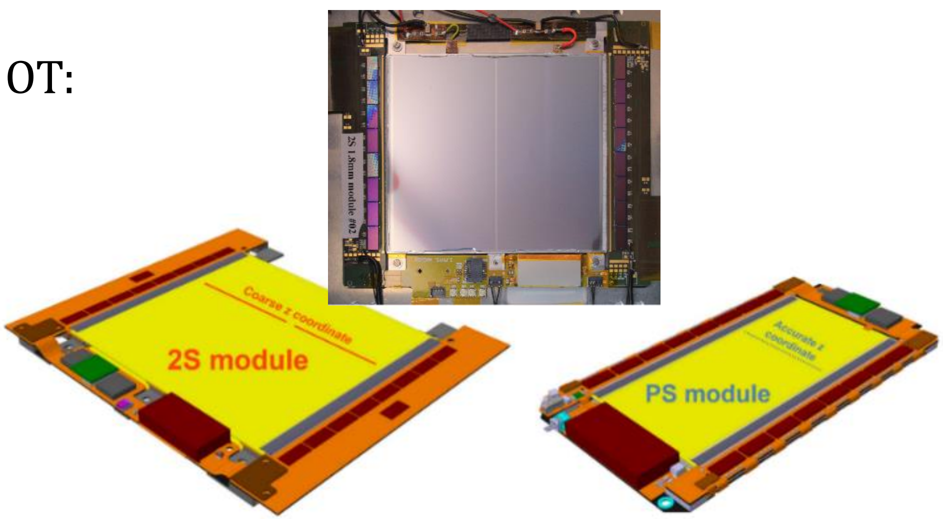

Trk TDR

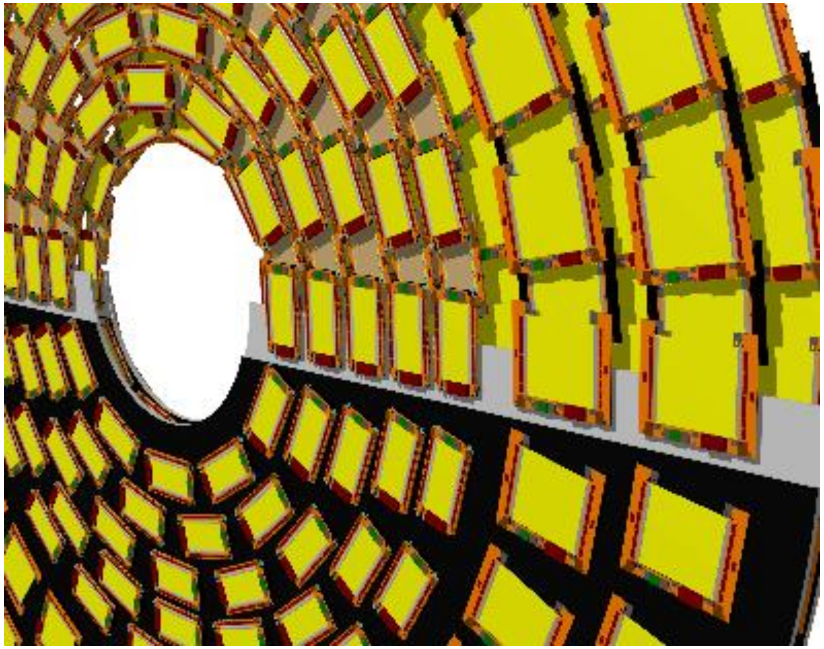

Tracking Upgrades

- Smaller pixel sensors for better granularity
- Particles hit more than 8 layers out to η = 3.5, and more than 6 to η = 4
- Better track separation, reduce hit merging in high energy jets
- Reduced material -- better routing of services around sub-detector interfaces

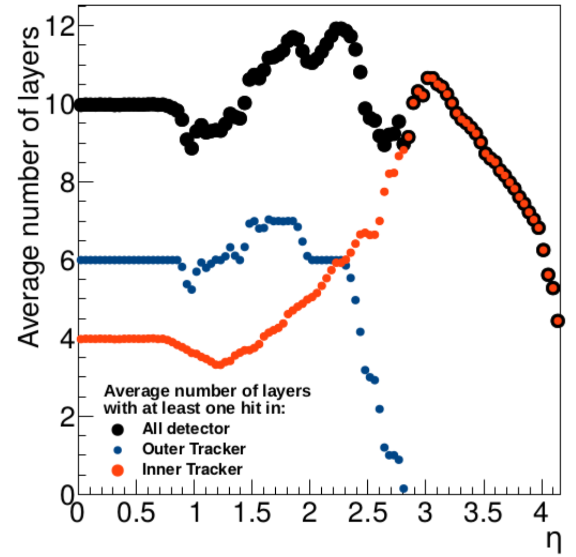

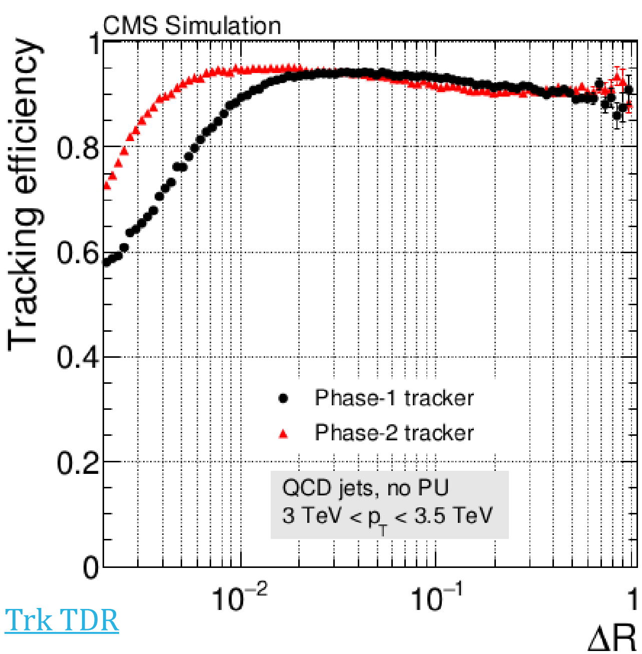

Trk TDR

Phase 1 → phase 2

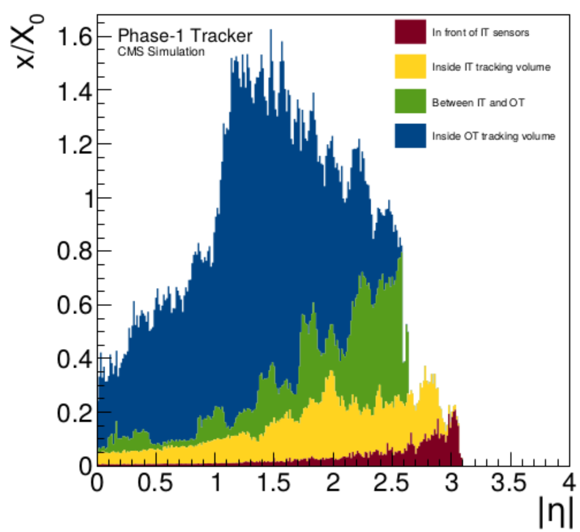

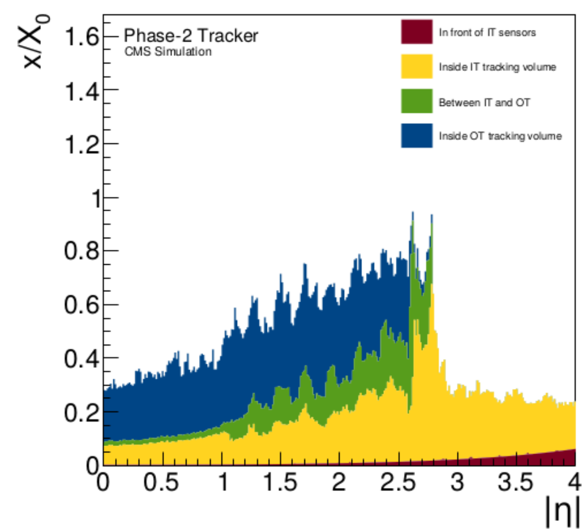

Tracking Upgrades

- Efficient track finding for L-1 trigger
- Stub-finding in 2-sensor modules
- 15k stubs @ 14 MHz, $p_T > 2$ GeV
- Goal is FPGA-only tracking

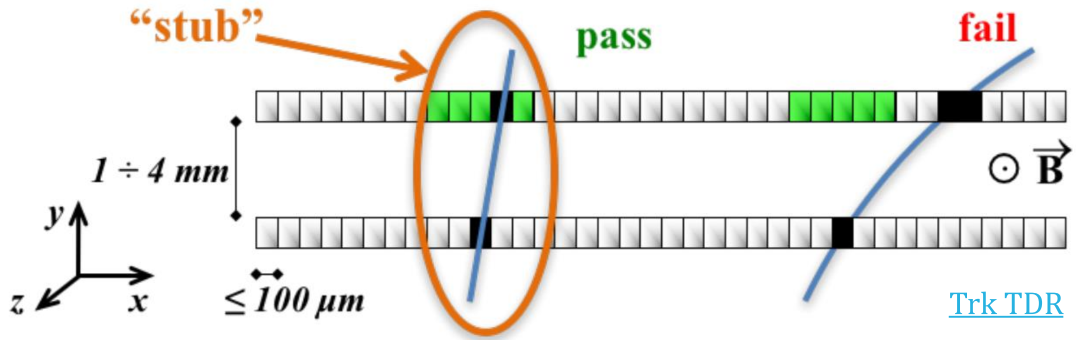

FPGA tracklet (stub-pair)
road search tracking

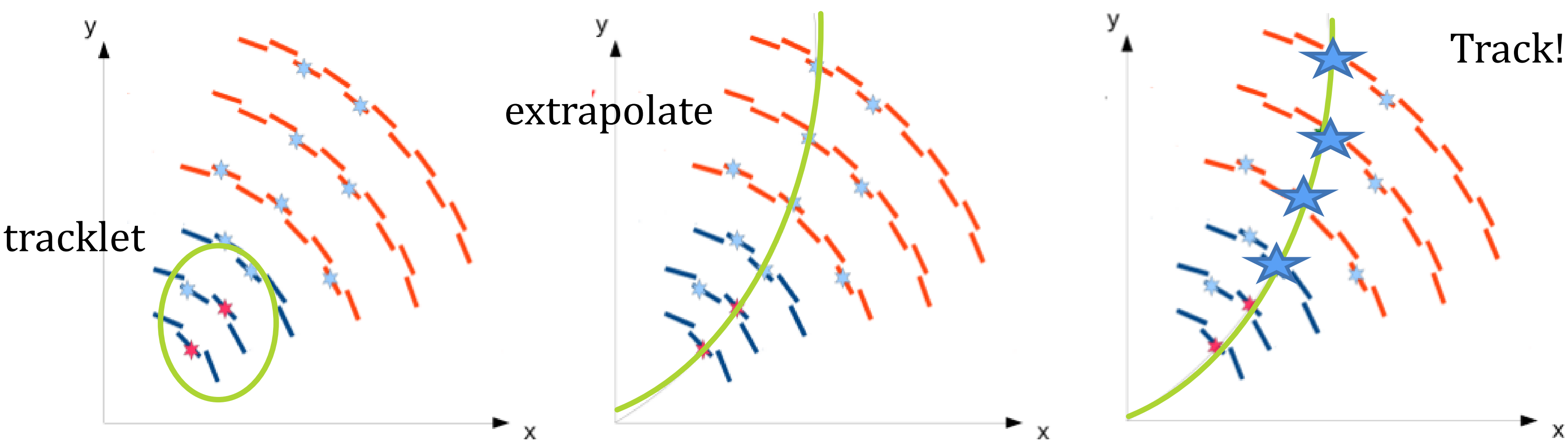

Tracking performance

- Momentum & IP resolution will improve
- Efficiency can maintained to 200 PU
- Vertex merging becomes an issue at high pileup
- Motivates including timing layer

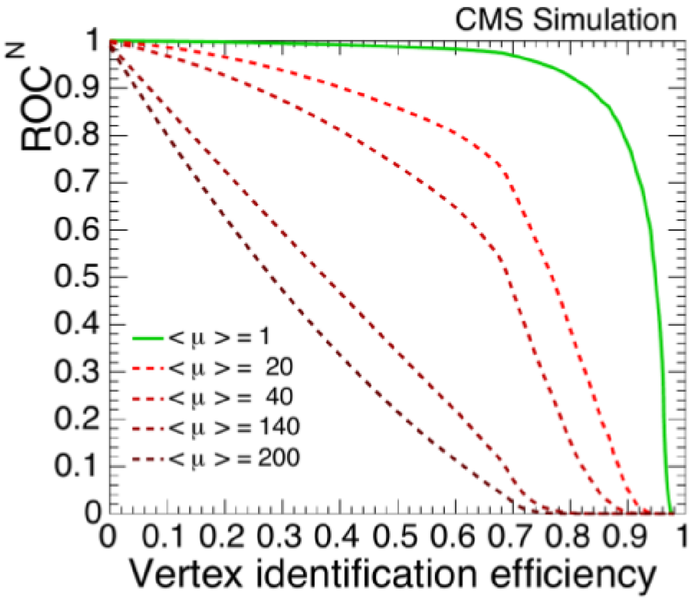

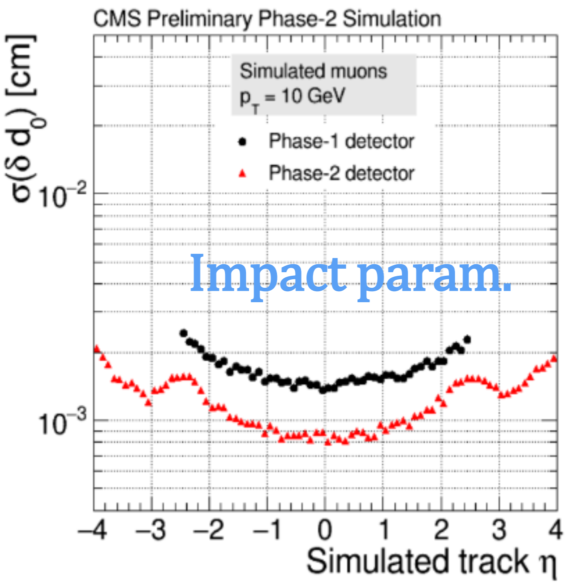

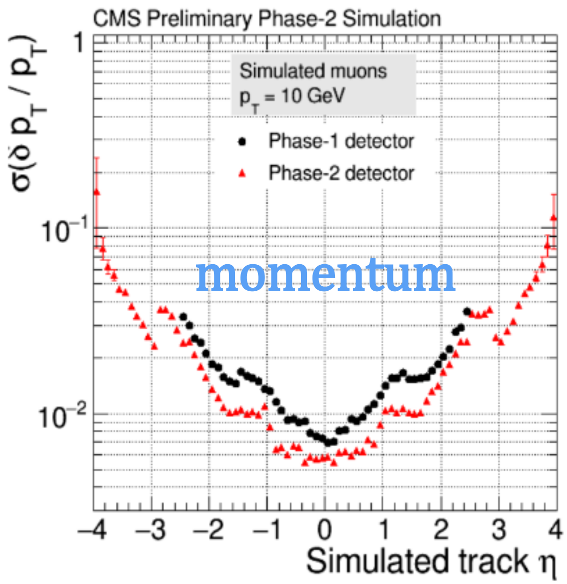

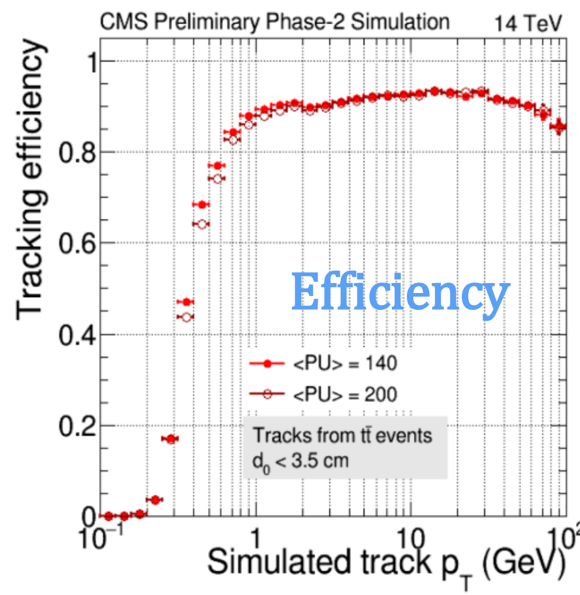

Trk TDR

MIP Timing Layer

- Fits between outer tracker and ECAL (barrel), and between tracker bulkhead and future HGCAL (endcap). Tight squeeze!
- **30-40 ps timing resolution for HL-LHC start**
- Adds p / K / π particle ID (backup)

[MTD TDR]

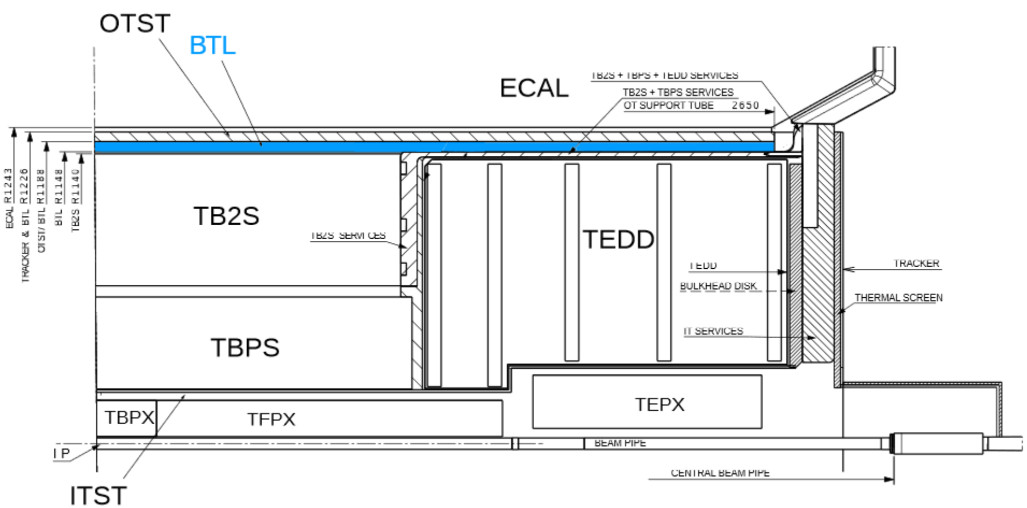

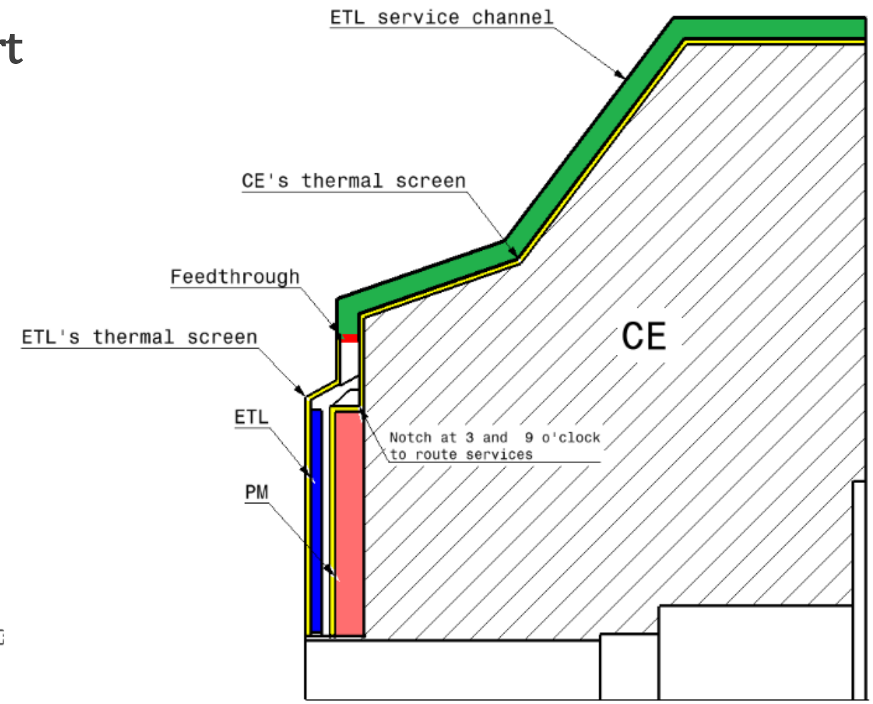

BTL: LYSO bars + SiPM readout:

- TK / ECAL interface: |η| < 1.45
- Inner radius: 1148 mm (40 mm thick)
- Length: ±2.6 m along z
- Surface ~38 m^2; 332k channels
- Fluence at 4 ab^{-1}: 2x10^{14} n_{eq}/cm^2

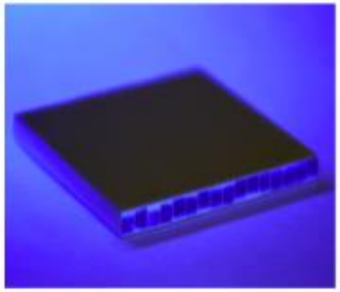

ETL: Si with internal gain (LGAD):

- On the CE nose: 1.6 < |η| < 3.0
- Radius: 315 < R < 1200 mm
- Position in z: ±3.0 m (45 mm thick)
- Surface ~14 m^2; ~8.5M channels
- Fluence at 4 ab^{-1}: up to 2x10^{15} n_{eq}/cm^2

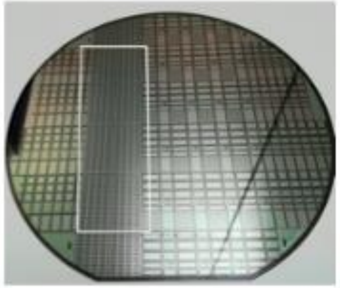

MIP Timing Layer

- Endcap: much higher fluence
- Low gain avalanche detectors
- 1.3 x 1.3 mm^2 pads in 16x32 arrays
- 2 ROCs to read 16x16 arrays

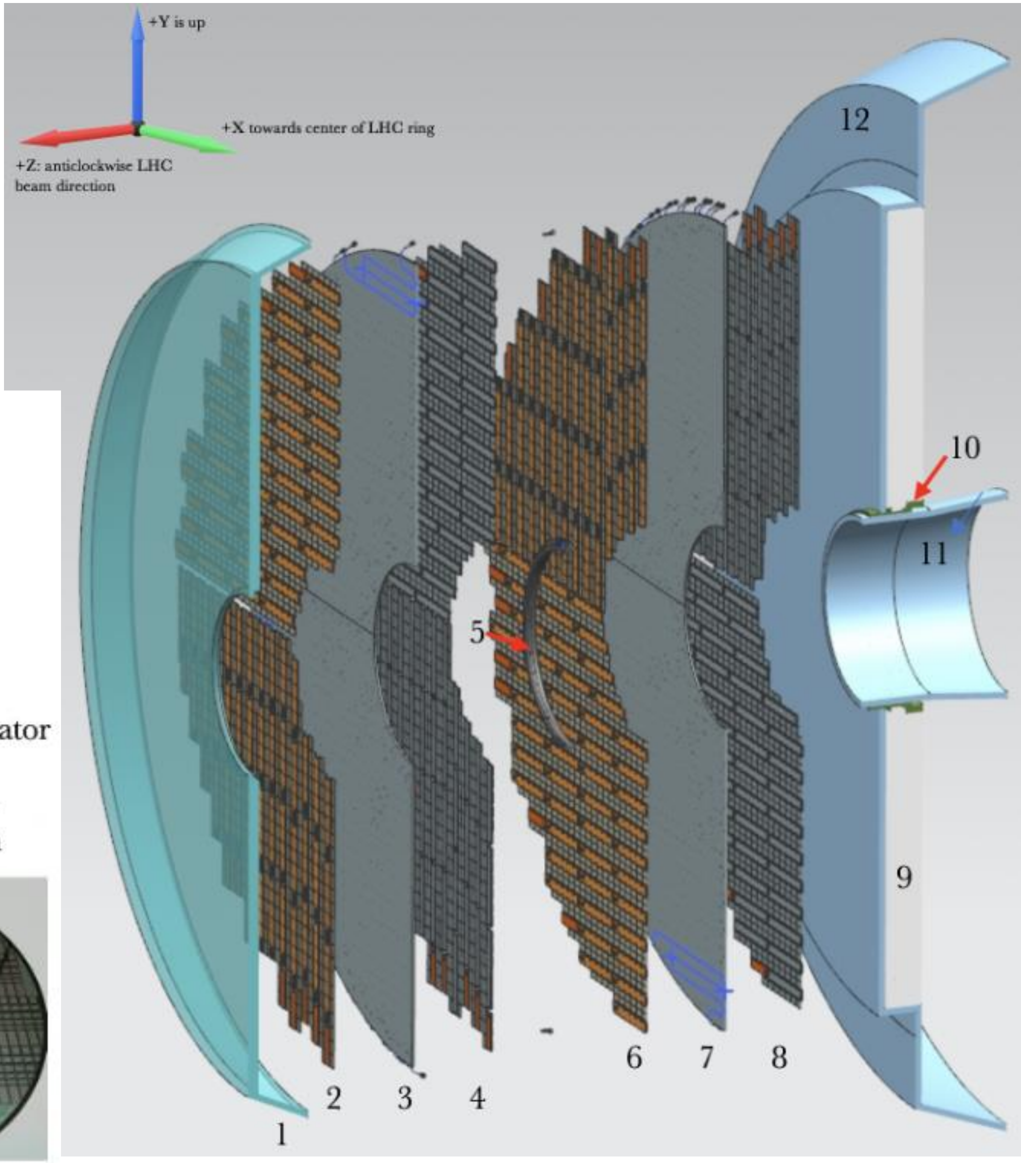

1: ETL Thermal Screen
2: Disk 1, Face 1
3: Disk 1 Support Plate
4: Disk 1, Face 2
5: ETL Mounting Bracket
6: Disk 2, Face 1
7: Disk 2 Support Plate
8: Disk 2, Face 2
9: HGCal Neutron Moderator
10: ETL Support Cone
11: Support cone insulation
12: HGCal Thermal Screen

MTD TDR

ETL: Si with internal gain (LGAD):
- On the CE nose: $1.6 < |\eta| < 3.0$
- Radius: 315 < R < 1200 mm
- Position in z: ±3.0 m (45 mm thick)
- Surface ~14 m^2; ~8.5M channels
- Fluence at 4 ab^{-1}: up to 2×10^{15} n_{eq}/cm^2

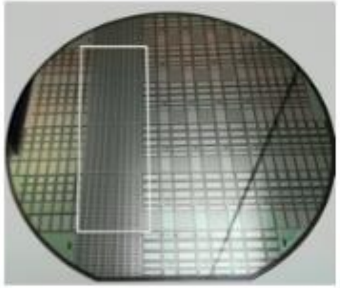

Calorimetry upgrades

- Electronics upgrades for barrel calorimeters to improve latency, add cluster timing capabilities, and lower the operating temperature
- **Radiation damage will cause large light losses in the endcaps**
  - Complete replacement required with more robust technology
- High granularity silicon endcap calorimeter – 3D shower images
  - Could allow triggering on displaced objects with large cτ

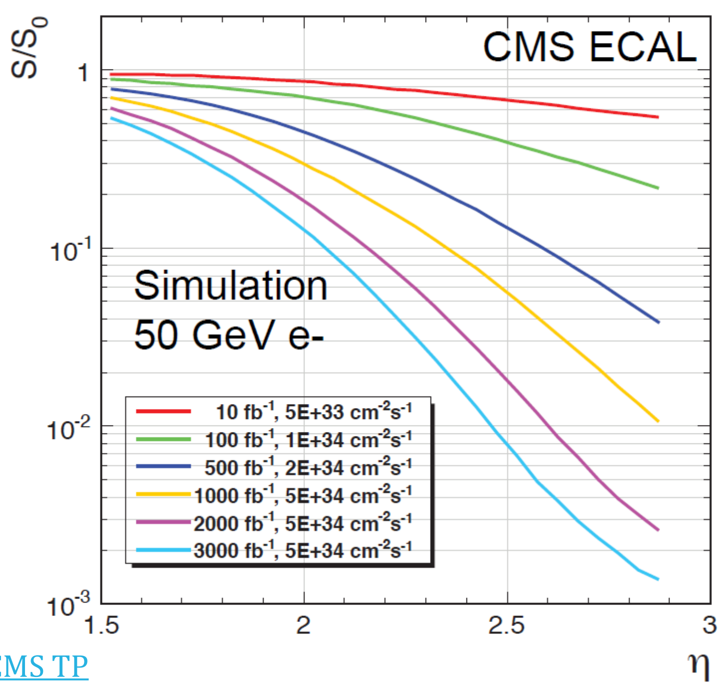

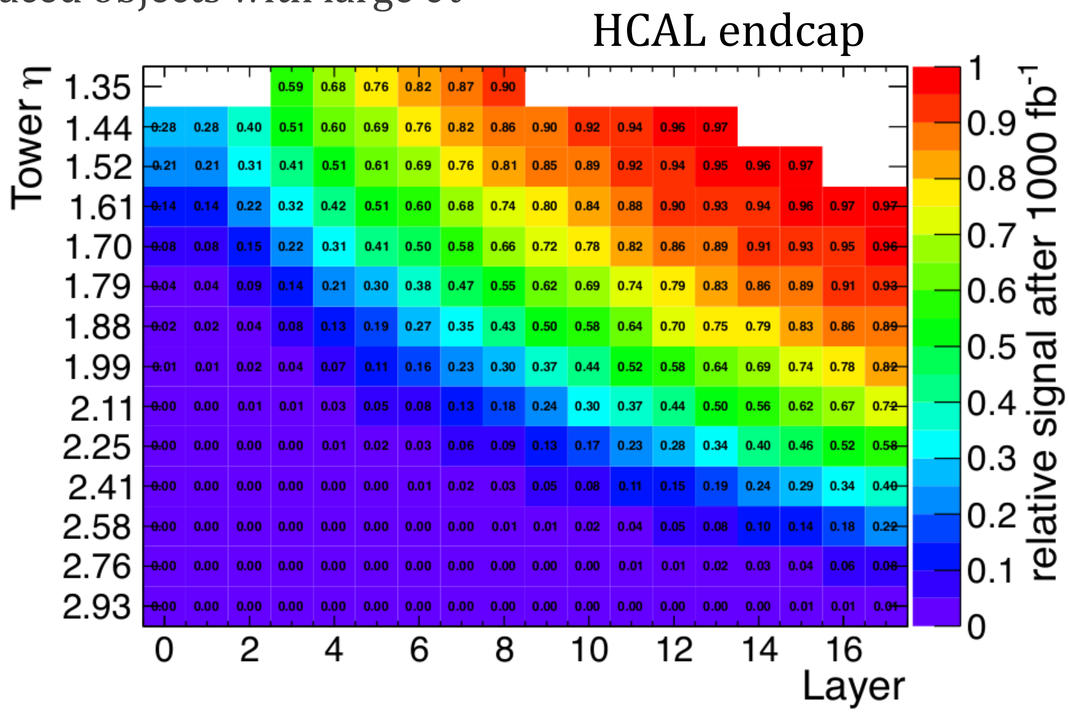

CMS TP

HG Encap Calorimeter

- **High granularity silicon endcap calorimeter – 3D shower images**
  - CE-E: Si sensors, tungsten/copper and lead/steel absorbers
  - CE-H: Si sensors, steel absorber
  - Si sensors → plastic scintillator where fluence is lower
  - Hexagonal sensors cooled to -30 C to minimize damage
  - Thinner sensors in regions of higher fluence

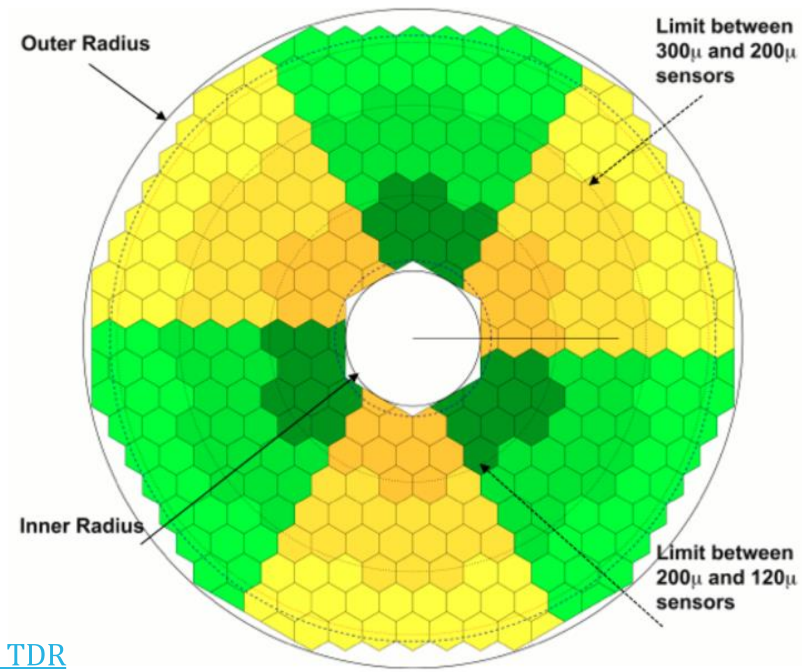

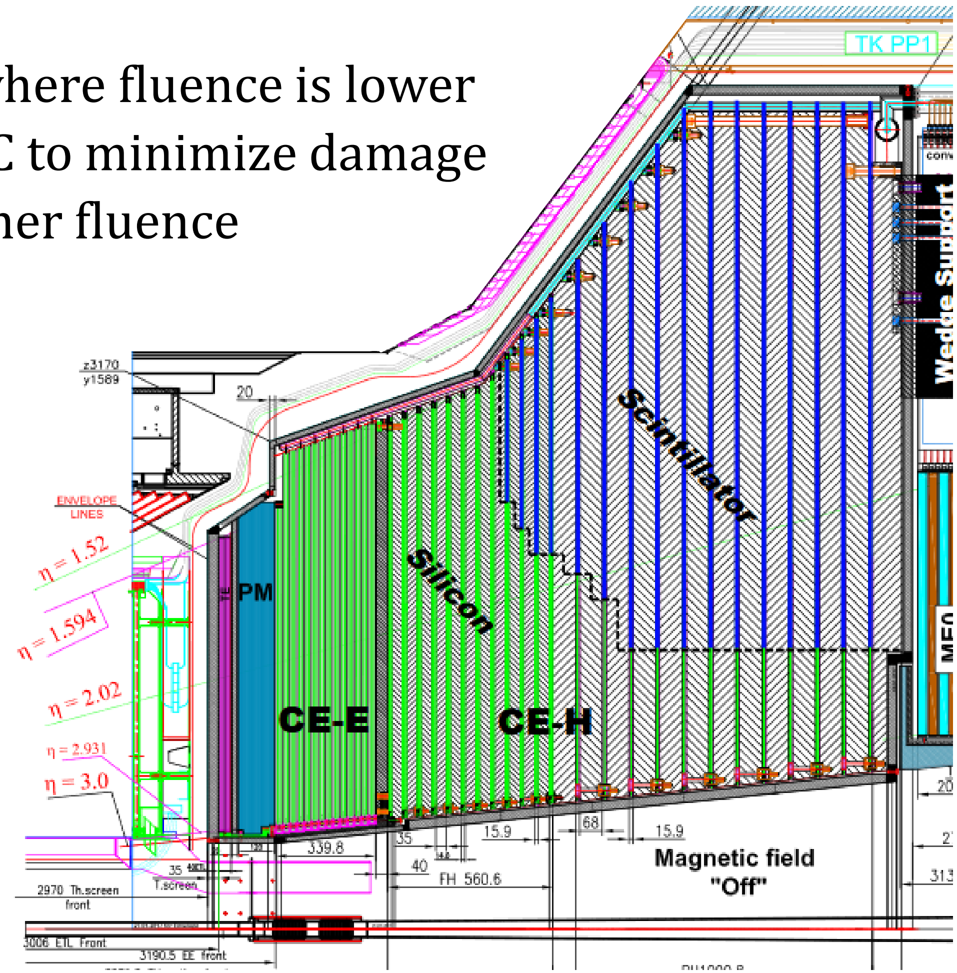

[CE TDR]

HGCAL silicon Module

- Hexagonal Si sensors with pads of ~1.2 cm^2 (thick) or 0.5 cm^2 (thin)
- Thinned p-type substrate, $$ but better against radiation-induced noise
- Diamond substructure for convenient readout and triggering
- Wirebonds drop through holes in the PCB where 3 Si pads intersect

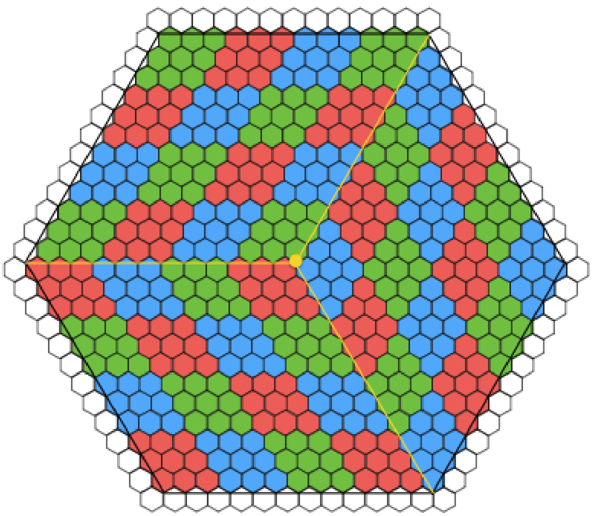

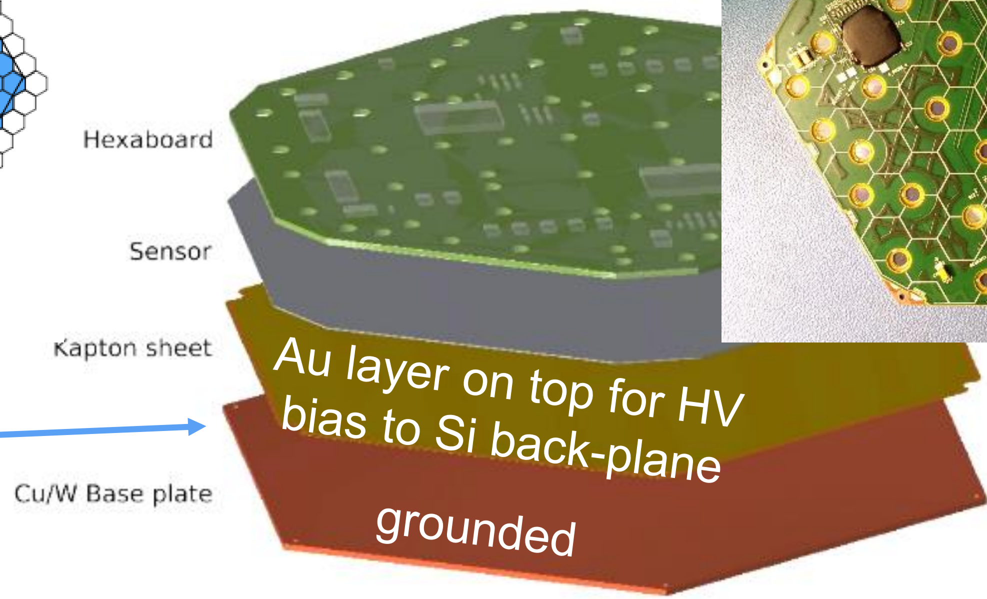

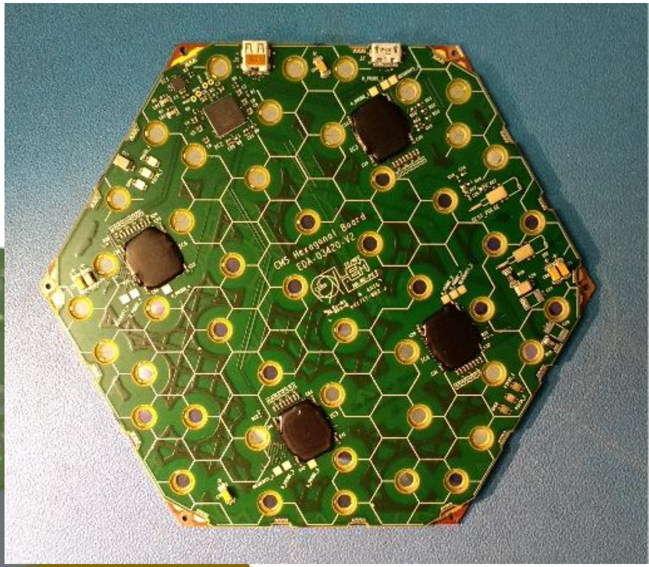

Corner cutouts expose mounting holes, allow wirebonds to Kapton

CE TDR

HGCAL scintillator

- This scintillator must last throughout the HL-LHC
- Current detector shows dose-rate-dependent chemical damage
- Considering polyvinyltoluene or polystyrene scintillator
- SiPM-on-tile technology
  - direct readout of light
  - SiPM in a dimple on the scintillator
  - Cell size of 4 through 32 cm^2

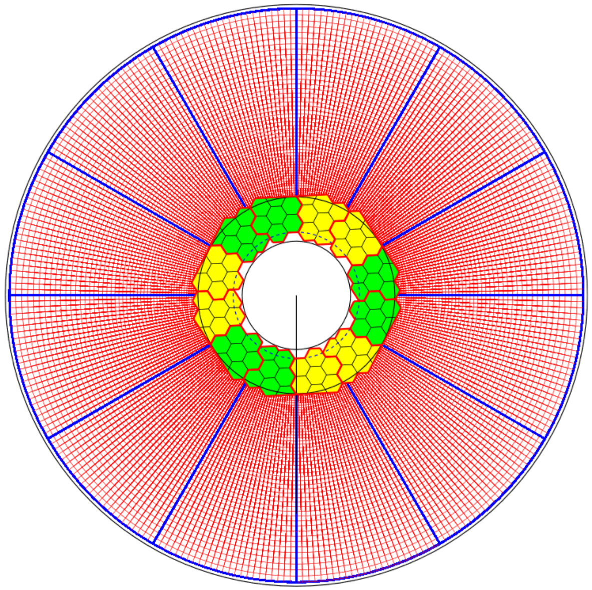

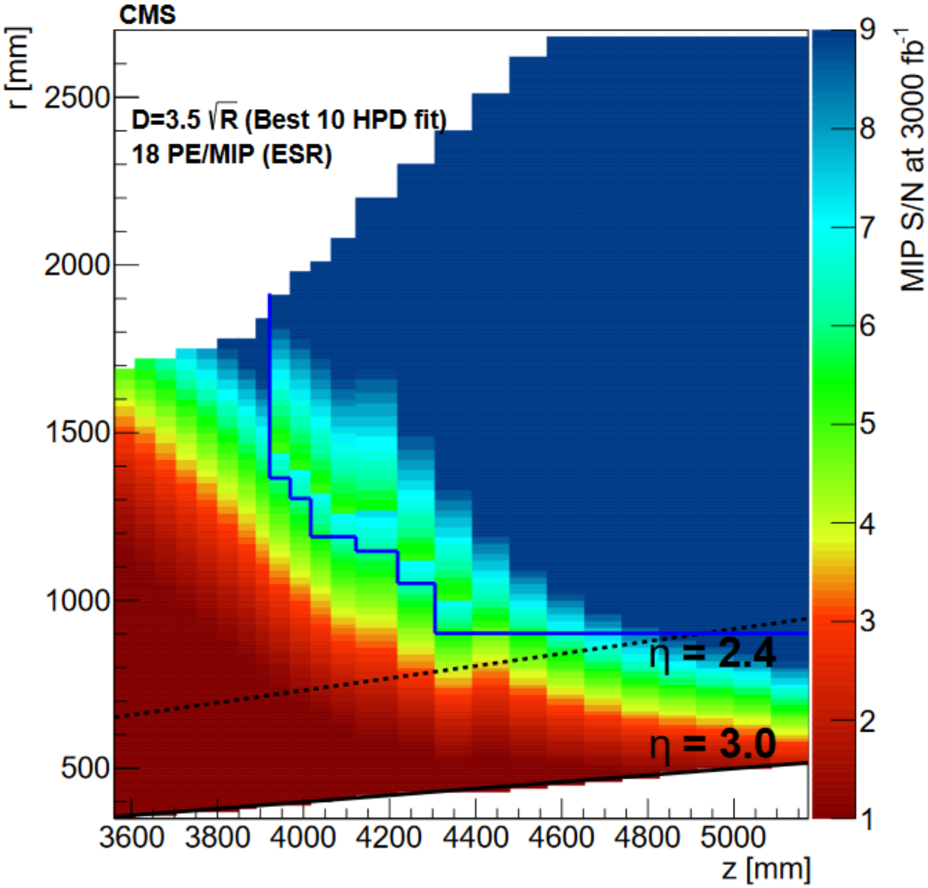

CE TDR

Muon Upgrades

- Current detectors will receive upgraded electronics
- New: forward gas electron multipliers and improved RPCs
- Standalone (no PV) muons in trigger up to $\eta = 2.4$
- Reliable triggering and offline measurement of muons up to $\eta = 2.8$

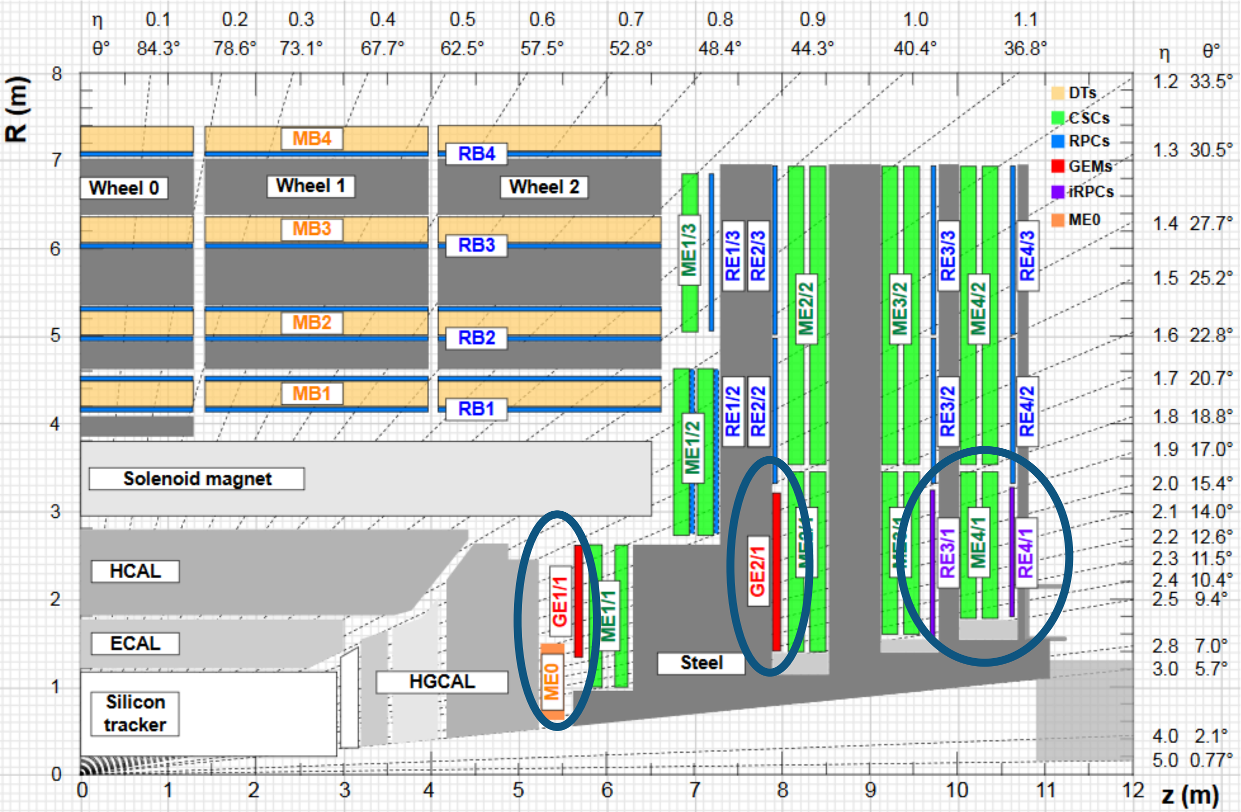

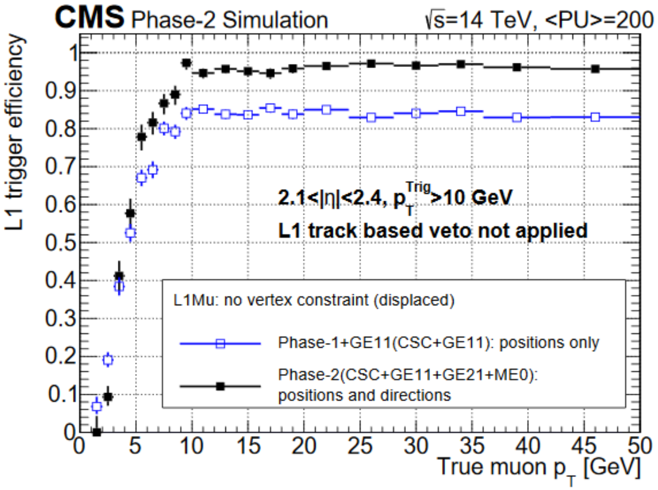

[Muon TDR](#)

Muon Upgrades

- Gas electron multipliers can handle hit rate of MHz/cm^2!
  - Better muon bending measurement within a station (up to 6 foils)
- Improved resistive plate chambers can handle HL-LHC rates
  - Faster electrode recovery (thinner), less charge (lower HV), better electronics
- Better spatial & time resolution, suppression of low p_T tracks

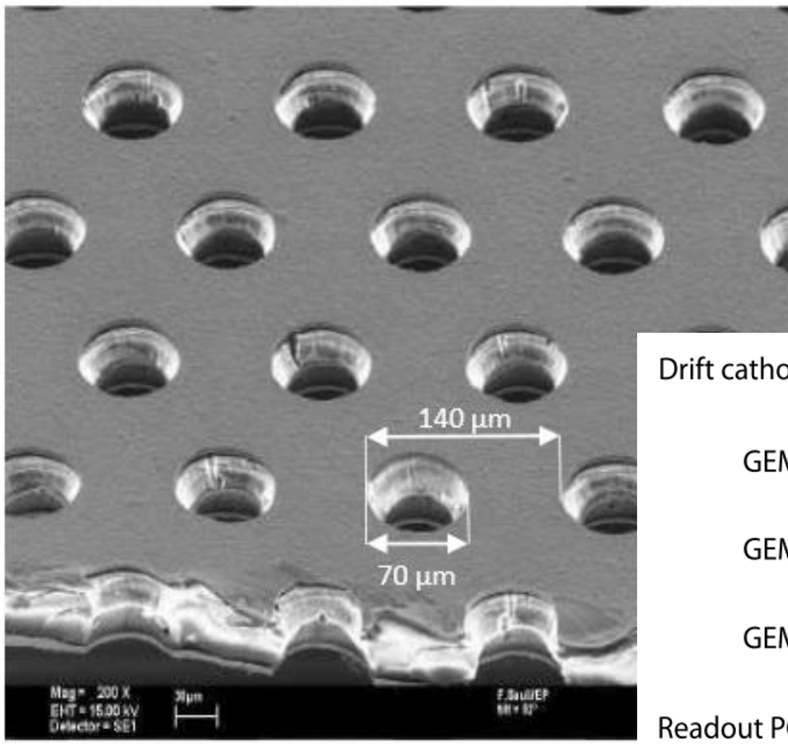

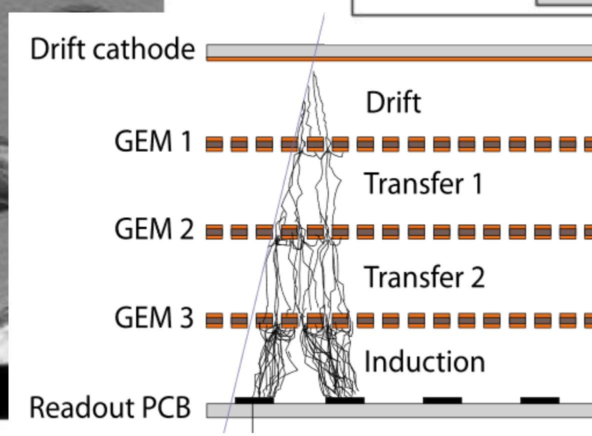

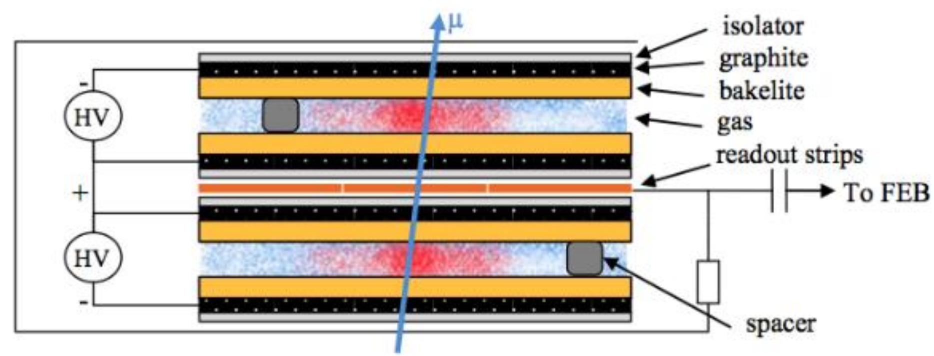

Muon TDR

Summary

- CMS Phase-2 program is progressing well with dedicated effort of many teams
- Technical Design Reports for Trackers, Muon Detectors, Barrel Calorimeter, Timing Layer, Endcap Calorimeters, L-1 Trigger available
- Critical improvements to triggering & reconstruction of all physics objects for good performance at 200 PU
- Physics case is extremely broad! Lots of attention given to signatures that are difficult with the current detectors such as triggering long-lived particles
- Exciting things are coming in the forward detector region! **CMS Phase-2 detectors may be appropriate for a FMS.**

Backup

Tracker modules

- Two pixel options: rectangular 25 x 100 microns or 50 x 50 microns
- Both effective after high fluence, rectangular currently preferred
- Also investigating 3D innermost layer option

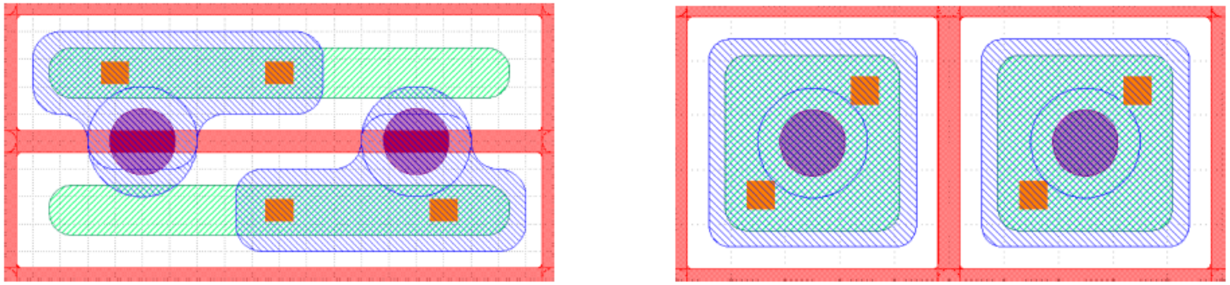

Figure 4.6: Drawing of two adjacent pixel cells for sensors from the HPK submission with pixel size $25 \times 100\,\mu m^2$ (left) and $50 \times 50\,\mu m^2$ (right). The n^+ implants are shown in green, the metal layers in blue, the p-stop areas in red, the contacts in orange, and the bump bond pads in purple.

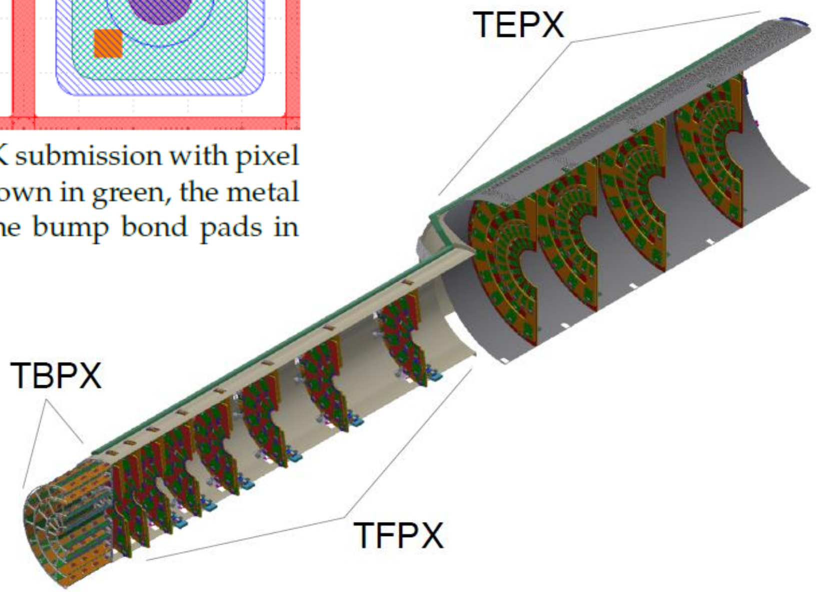

Figure 4.2: Perspective view of one quarter of the Inner Tracker, showing the TBPX ladders and TFPX and TEPX dees inside the supporting structures. The pixel modules are shown as orange elements in TBPX and as green elements in TFPX and TBPX. The dees are depicted as red and orange surfaces.

Tracker modules

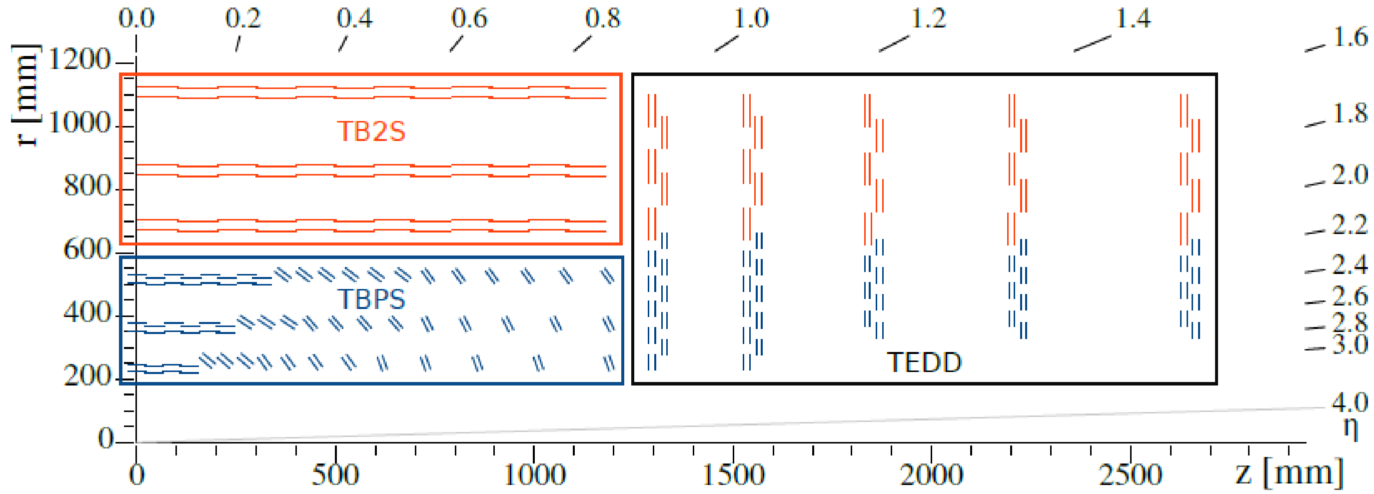

Figure 3.1: Sketch of one quarter of the Outer Tracker in *r-z* view. Blue (red) lines represent PS (2S) modules. The three sub-detectors, named TBPS, TB2S, and TEDD, are indicated. All overlapping layers are shown separately, while in Fig. 2.3 the mean positions are shown.

Table 3.3: Dimensions and quantities of the three sensor types used in the Outer Tracker. All dimensions are given in micrometres. The active area is defined as the area enclosed within the centre line between the outermost strip implant or pixel implant and the bias ring implant. At this transition approximately half of the charge generated by a particle is lost to the bias ring. The percentage of spares is larger for the PS-p sensors as compared to the strip sensors, as the PS-p sensors will undergo bump bonding.

Sensor	Outer		Active		Strip/Pixel		Quantity	Quantity
name	width	length	width	length	pitch	length	needed	with spares
2S	94 183	102 700	91 440	100 548	90	50 274	15 360	17 660 (+15%)
PS-s	98 140	49 160	96 000	46 944	100	23 472	5 616	6 460 (+15%)
PS-p	98 740	49 160	96 000	46 944	100	1 467	5 616	6 740 (+20%)

Tracker modules

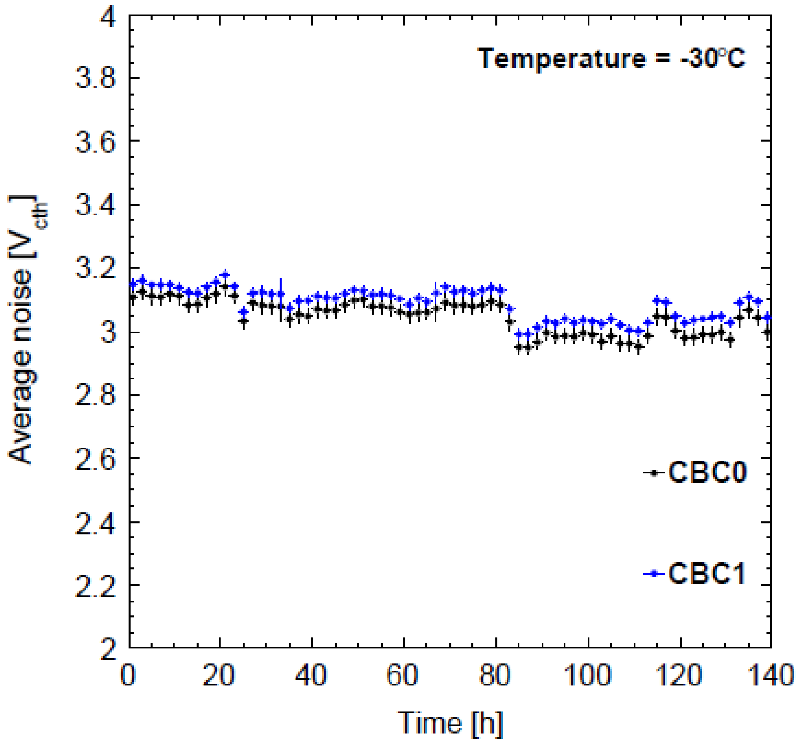

Sensor noise after time at -30C

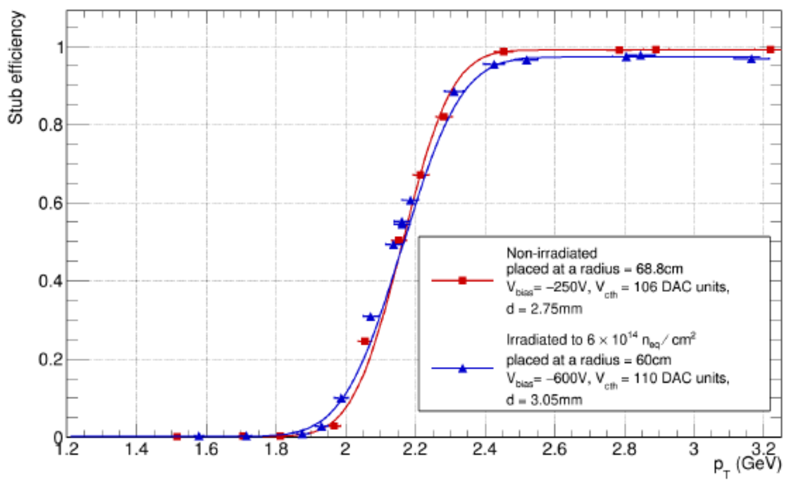

Figure 3.21: Stub reconstruction efficiency for a non-irradiated (red) and an irradiated (blue) 2S mini-module. The mini-module was irradiated to a fluence of $6 \times 10^{14}\,n_{eq}/cm^2$. The variable V_{cth} refers to the threshold setting, while d is the sensor spacing. The thresholds used correspond to about 4900 and 3500 electrons for the unirradiated and irradiated module, respectively. Radii of 69 cm and 60 cm were used for the calculation of the p_T from the tilt angle of the non-irradiated and irradiated module, respectively (Section 9.2.5.3). The different radii compensate for the fact that the modules had different sensor spacing but were operated with the same stub acceptance window.

Hit occupancy

Figure 6.3: Hit occupancy, defined as the fraction of channels containing a digitized hit, as a function of η for all layers and double-discs of the Inner Tracker (top) and Outer Tracker (bottom), for $t\bar{t}$ events with a pileup of 200 events. For the Outer Tracker, the occupancies in strip sensors and macro-pixel sensors are shown by filled and unfilled markers, respectively.

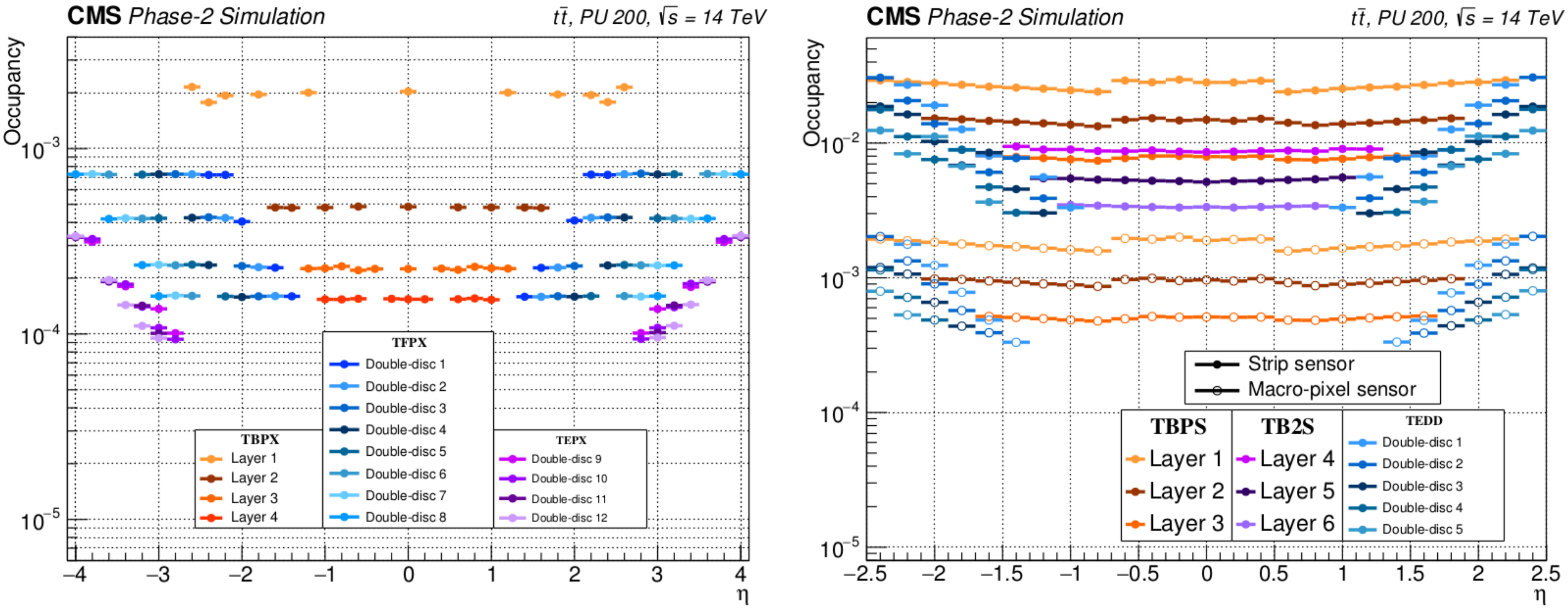

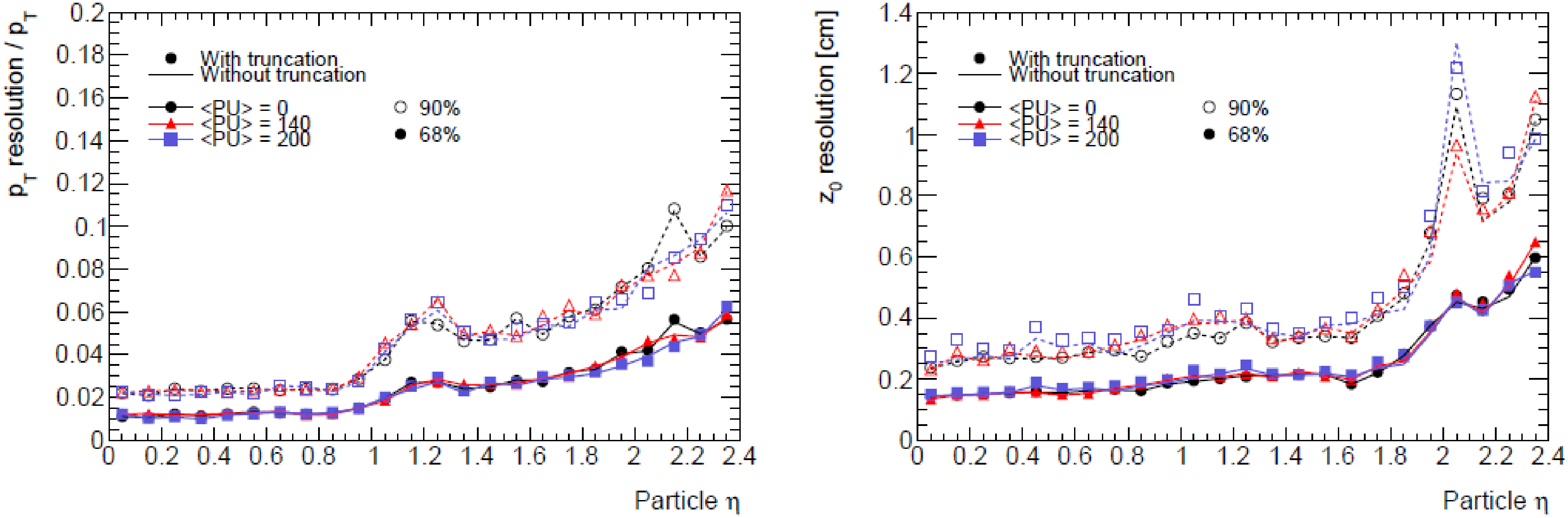

Figure 6.8: Relative p_T resolution (left) and z_0 resolution (right) versus pseudorapidity for muons in $t\bar{t}$ events with zero (black dots), 140 (red triangles), and 200 (blue squares) pileup events on average. Results are shown for scenarios in which truncation effects are (markers) or are not (lines) considered in the emulation of L1 track processing. The resolutions correspond to intervals in the track parameter distributions that encompass 68% (filled markers and solid lines) or 90% (open markers and dashed lines) of all tracks with $p_T > 3\,\mathrm{GeV}$.

tracking

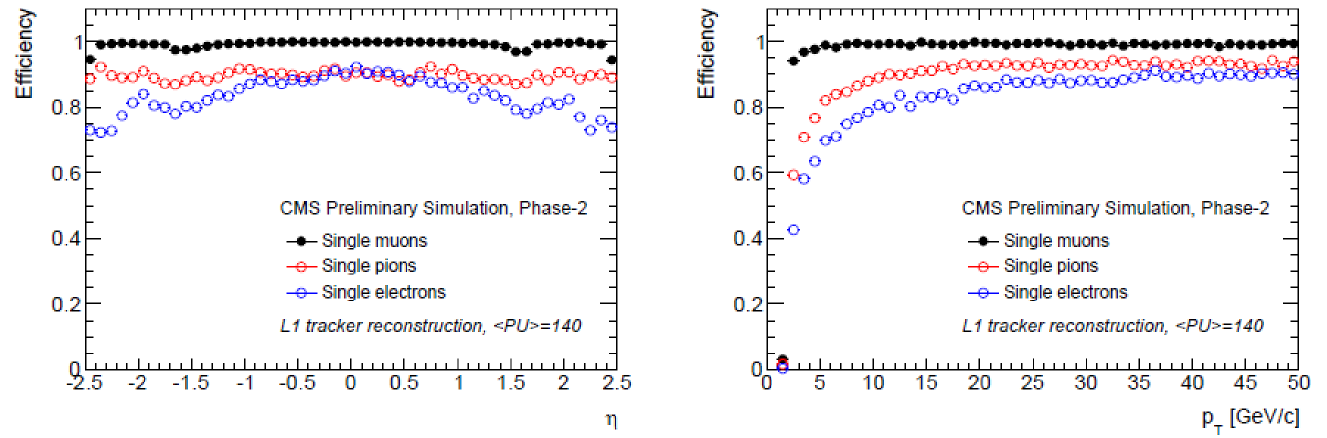

Figure 2.25: Efficiency for L1 track reconstruction as a function of η (left) and p_T (right) for muons, pions, and electrons.

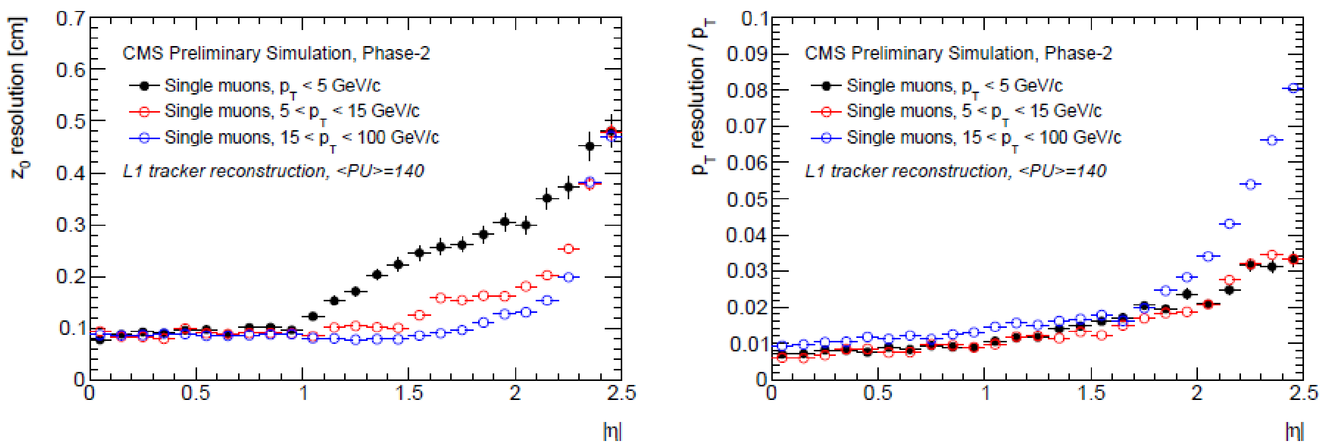

Figure 2.26: Resolution in z_0, and relative resolution in p_T for the L1 track reconstruction of single muons as function of η for different p_T ranges.

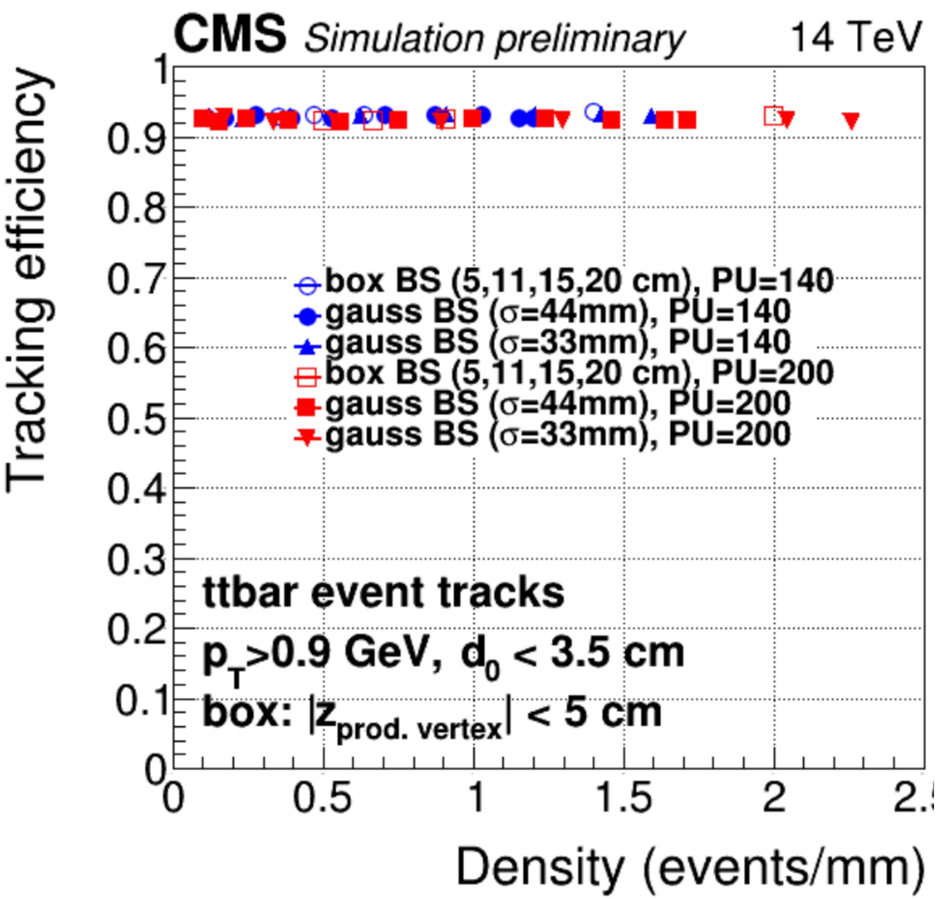
CMS Simulation preliminary
14 TeV
Tracking efficiency
box BS (5,11,15,20 cm), PU=140
gauss BS (σ=44mm), PU=140
gauss BS (σ=33mm), PU=140
box BS (5,11,15,20 cm), PU=200
gauss BS (σ=44mm), PU=200
gauss BS (σ=33mm), PU=200
ttbar event tracks
p_T>0.9 GeV, d_0 < 3.5 cm
box: |z_prod. vertex| < 5 cm
Density (events/mm)

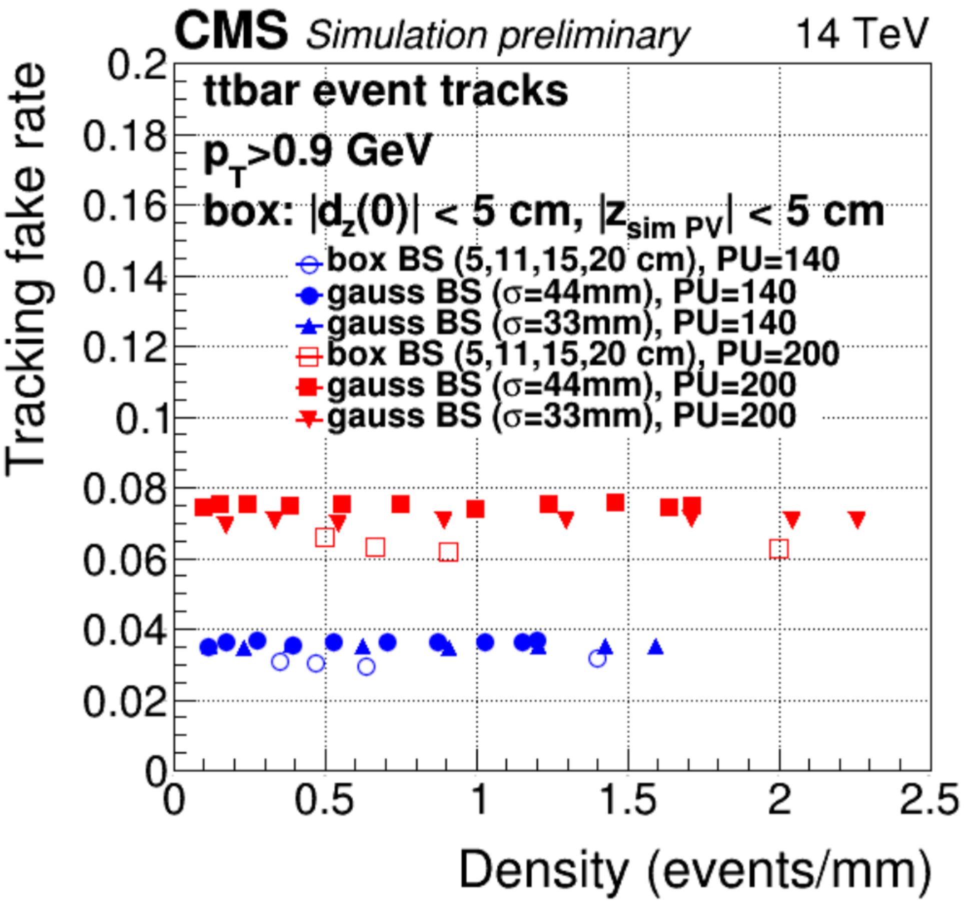
CMS Simulation preliminary
14 TeV
Tracking fake rate
ttbar event tracks
p_T>0.9 GeV
box: |d_z(0)| < 5 cm, |z_sim PV| < 5 cm
box BS (5,11,15,20 cm), PU=140
gauss BS (σ=44mm), PU=140
gauss BS (σ=33mm), PU=140
box BS (5,11,15,20 cm), PU=200
gauss BS (σ=44mm), PU=200
gauss BS (σ=33mm), PU=200
Density (events/mm)

MIP Timing Layer

- Separate vertices in time as well as space for 4D reconstruction
- 30-40 ps resolution for HL-LHC start
- Vertexing conditions similar to Run 2 in each ~30 ps time window

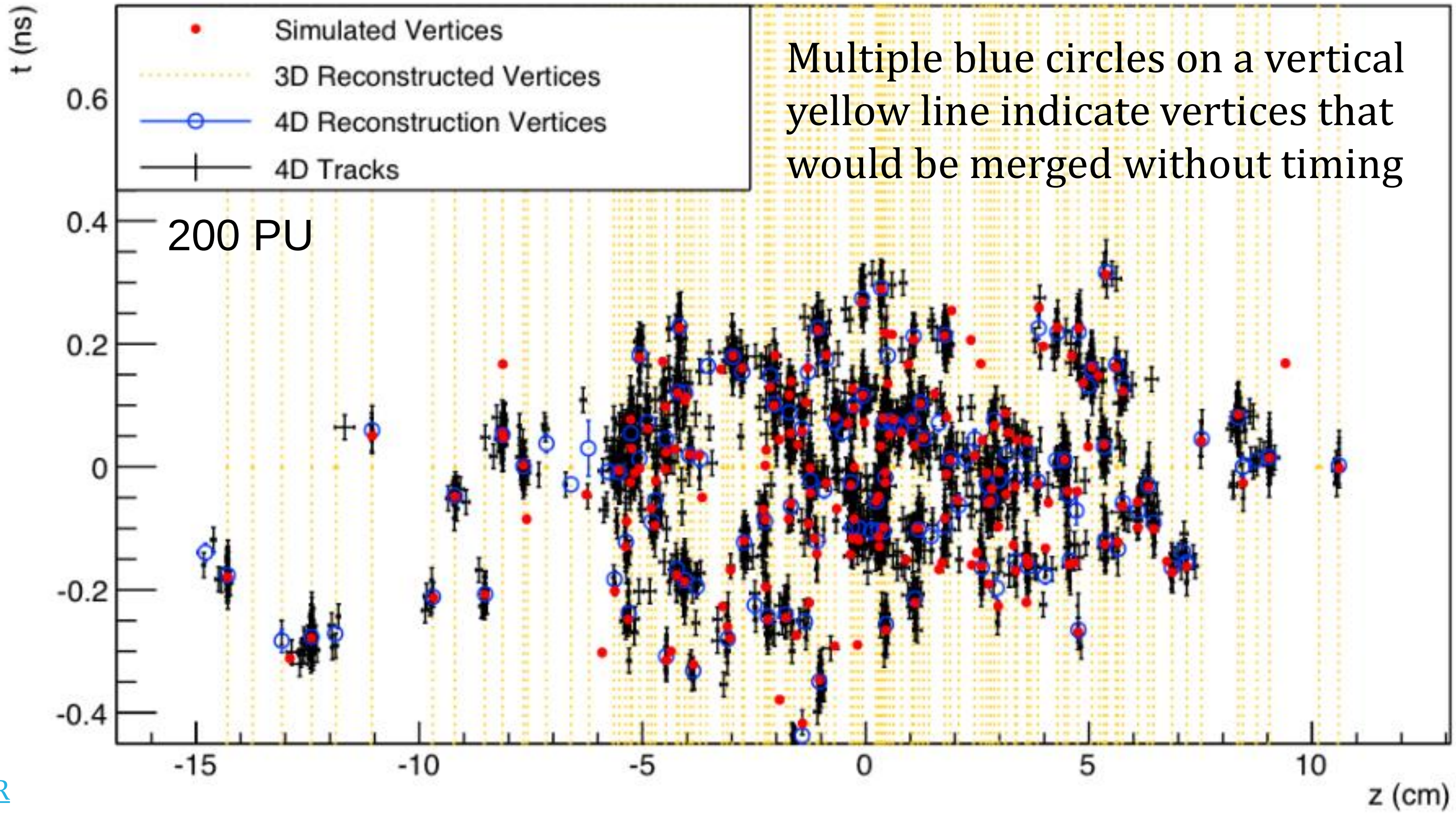

Multiple blue circles on a vertical yellow line indicate vertices that would be merged without timing

MTD TDR

Vertexing performance

- Separate vertices in time as well as space for 4D reconstruction
- 30-40 ps resolution for HL-LHC start
- **Significant reduction of pileup tracks associated to the PV**
- Benefits for tau, photon, b identification. Adds time-of-flight ID

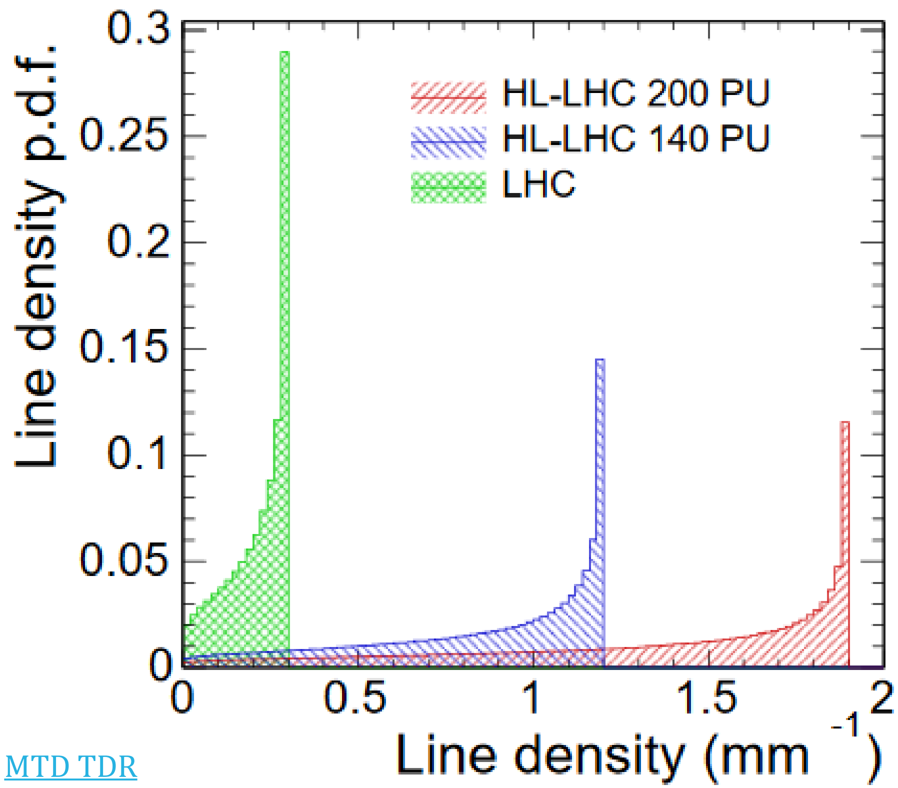

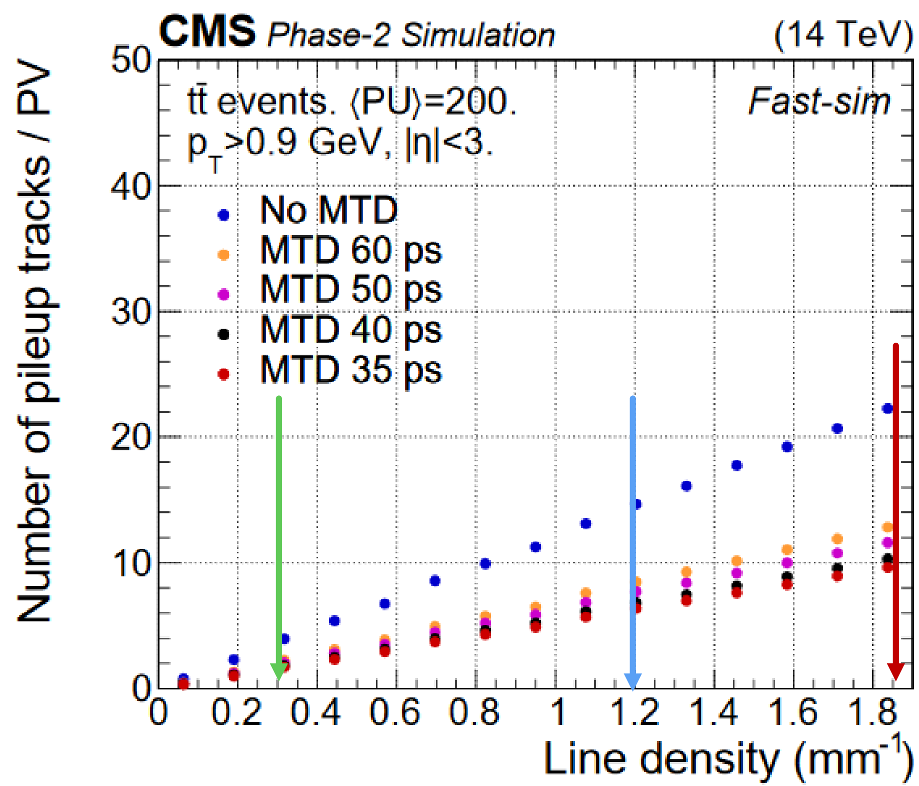

[MTD TDR]

Particle ID

- Time-of-flight-based particle ID K/p/pi

[MTD TDR]

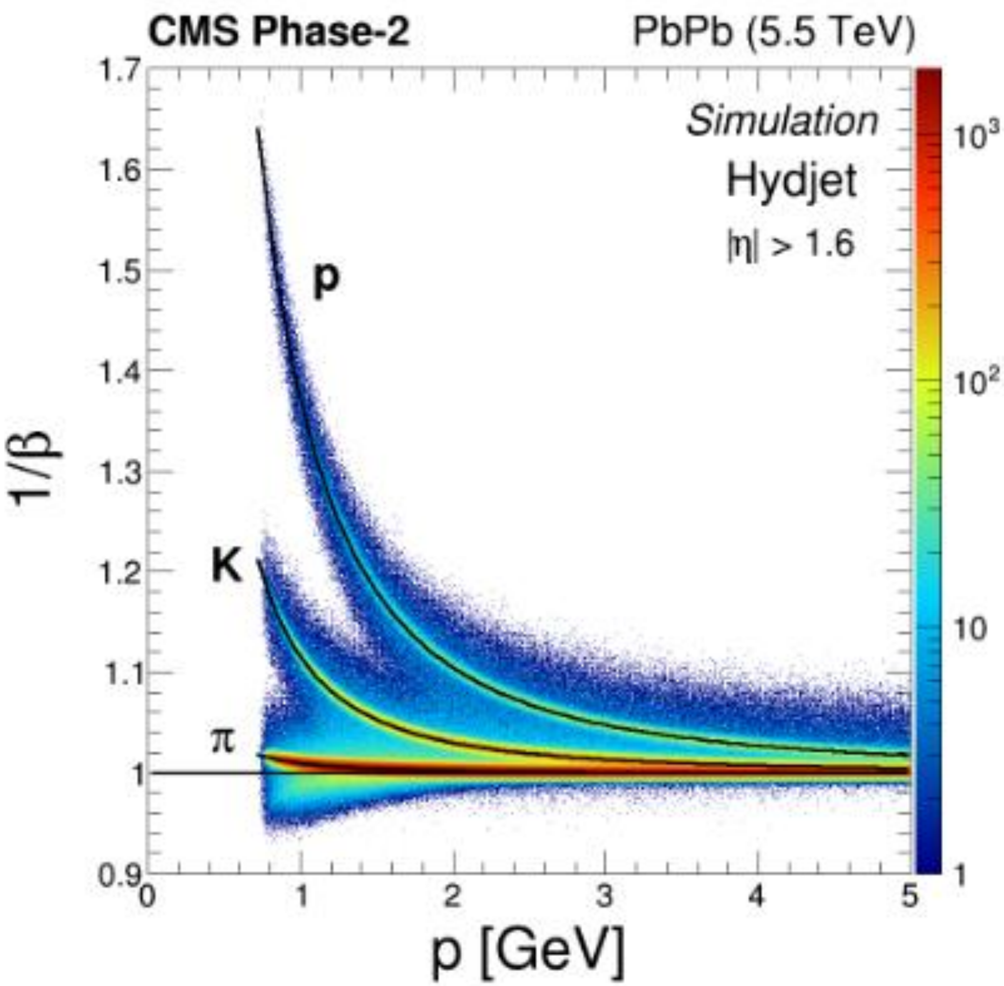

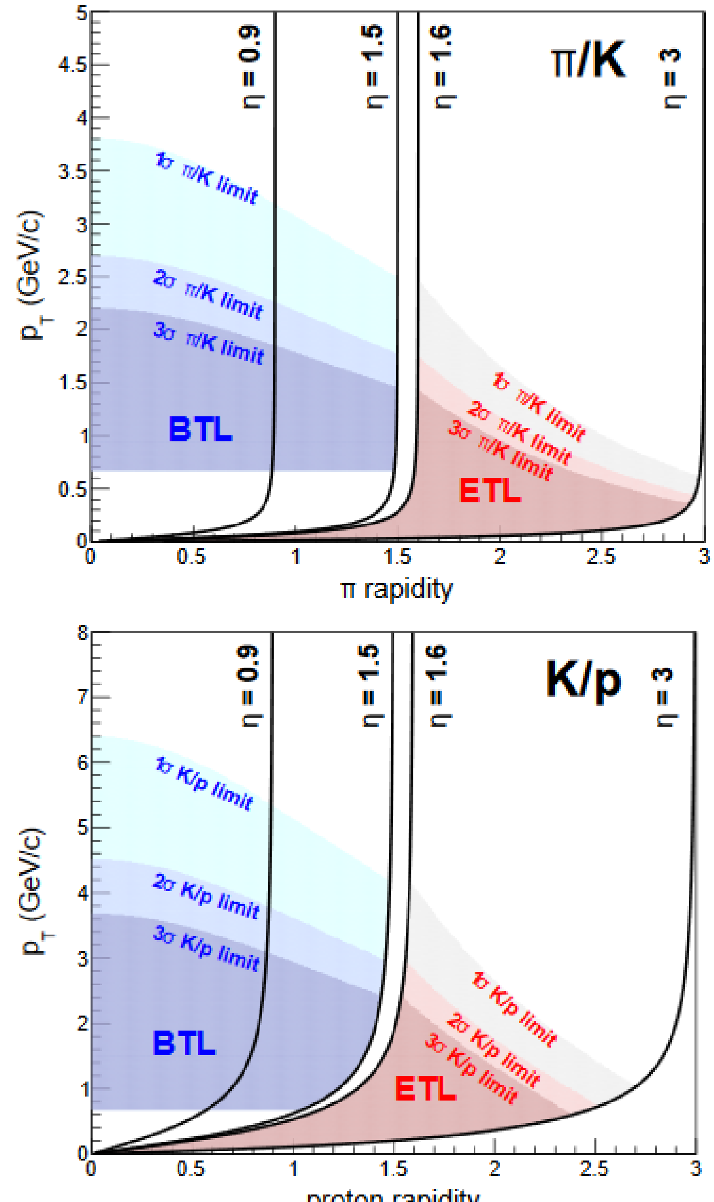

Endcap timing layer

MTD TDR

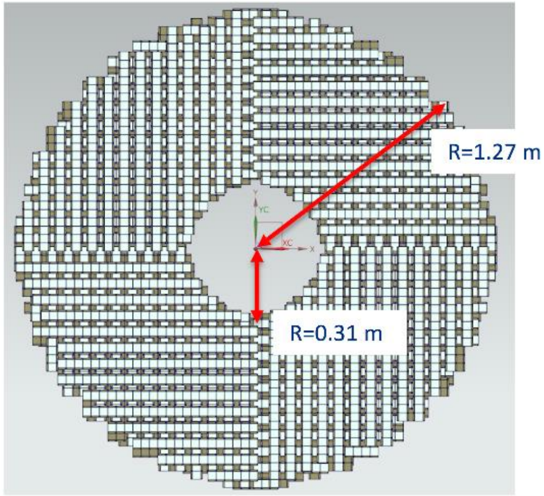

Figure 3.3: Sensor placement on one face of a disk. The modules are arranged in an $x-y$ layout, with readout channels placed between them to host powering and readout circuitry and provide cable servicing.

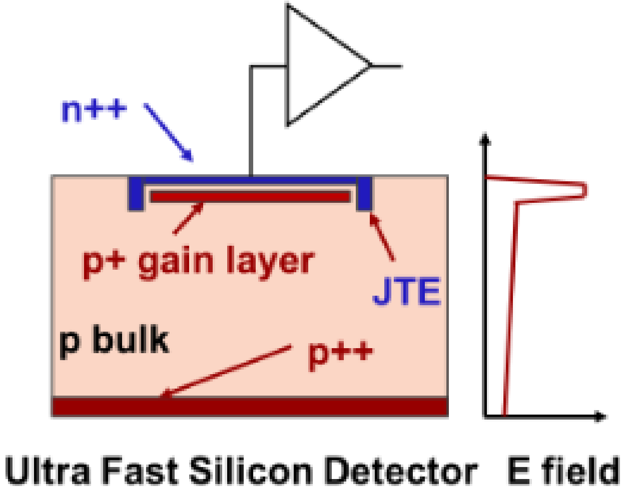

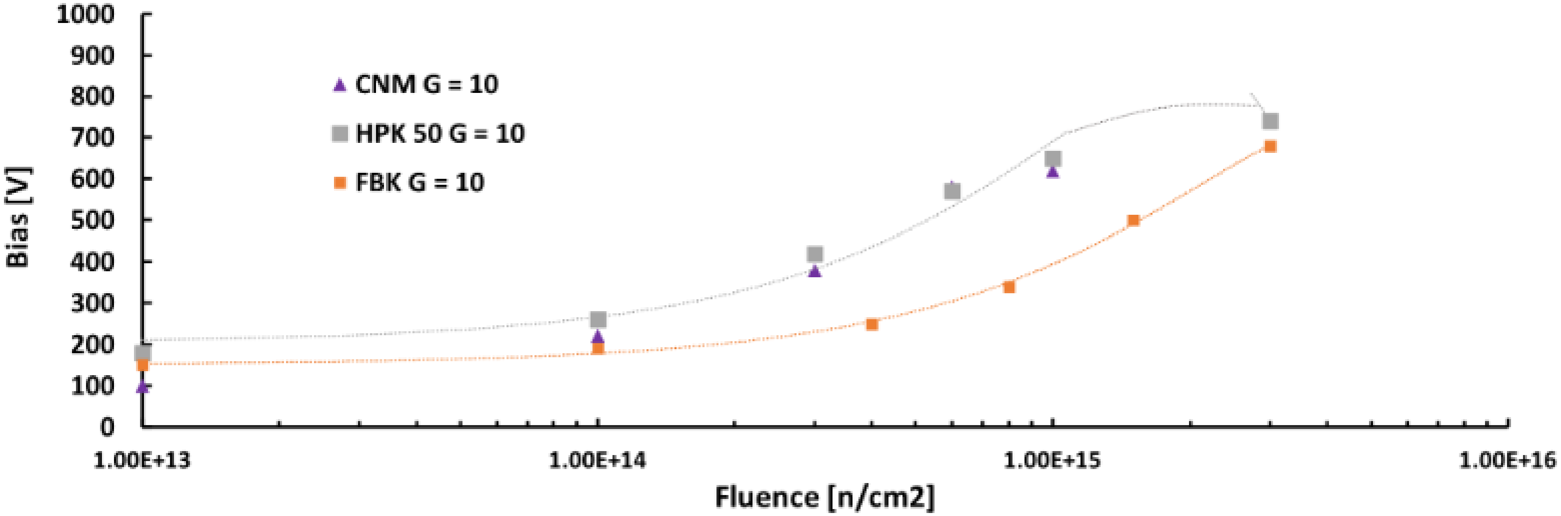

Endcap timing layer

MTD TDR

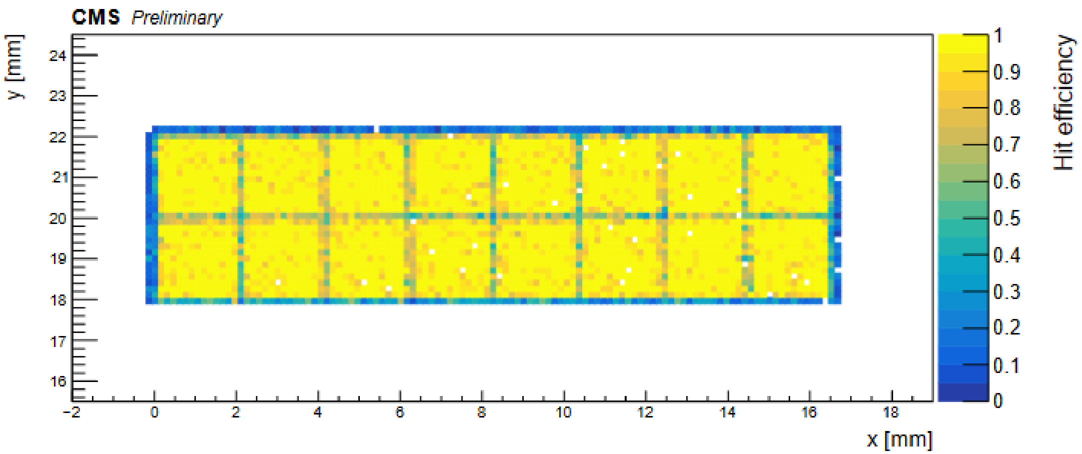

1: AlN module cover
2: LGAD sensor
3: ETL ASIC
4: Mounting film
5: AlN carrier
6: Mounting film
7: Mounting screw
8: Front-end hybrid
9: Adhesive film
10: Readout connector
11: High voltage connector
12: LGAD bias voltage wirebond
13: ETROC wirebonds

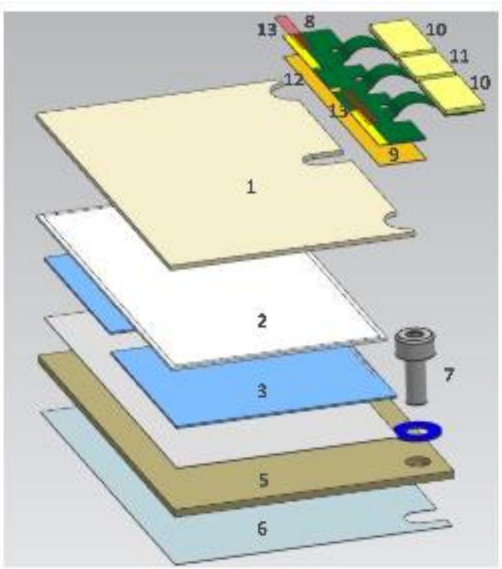

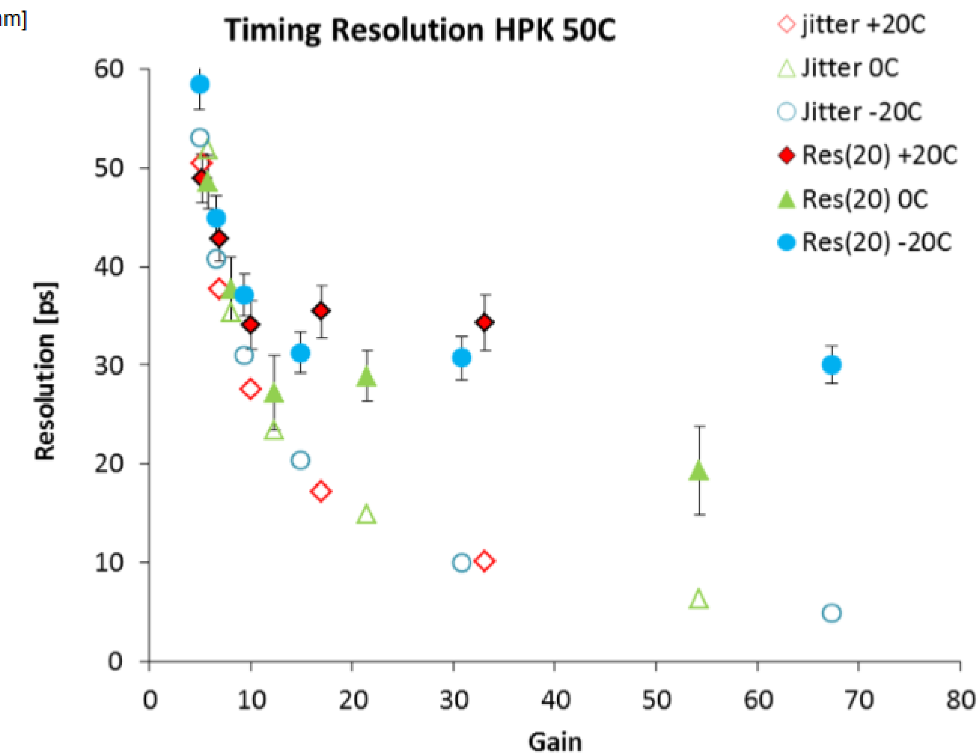

HCAL light loss

HCAL Barrel light loss

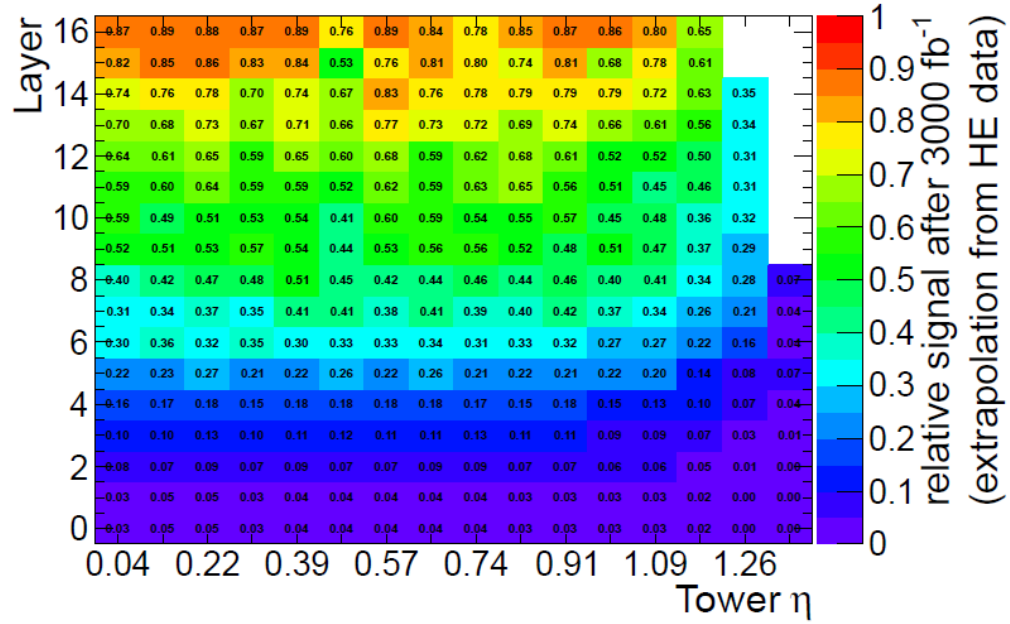

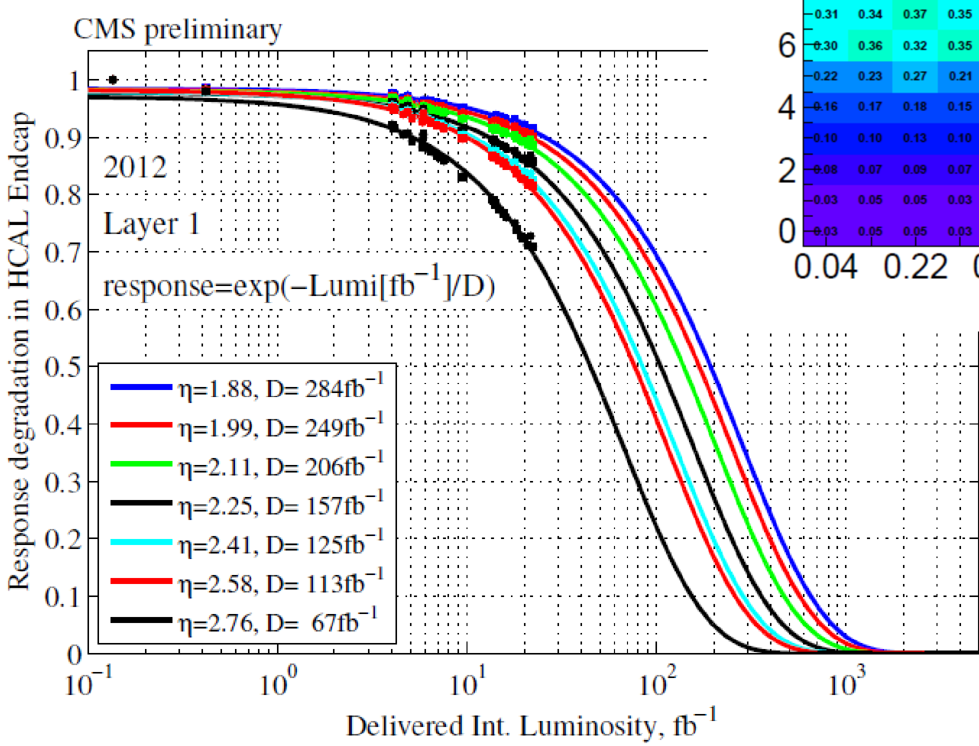

Figure 3.8: Fraction decrease of light signal from the first layer of HE as a function of accumulated luminosity for different values of the tile position (η), along with a fit to an exponential

CMS TP

CE structure

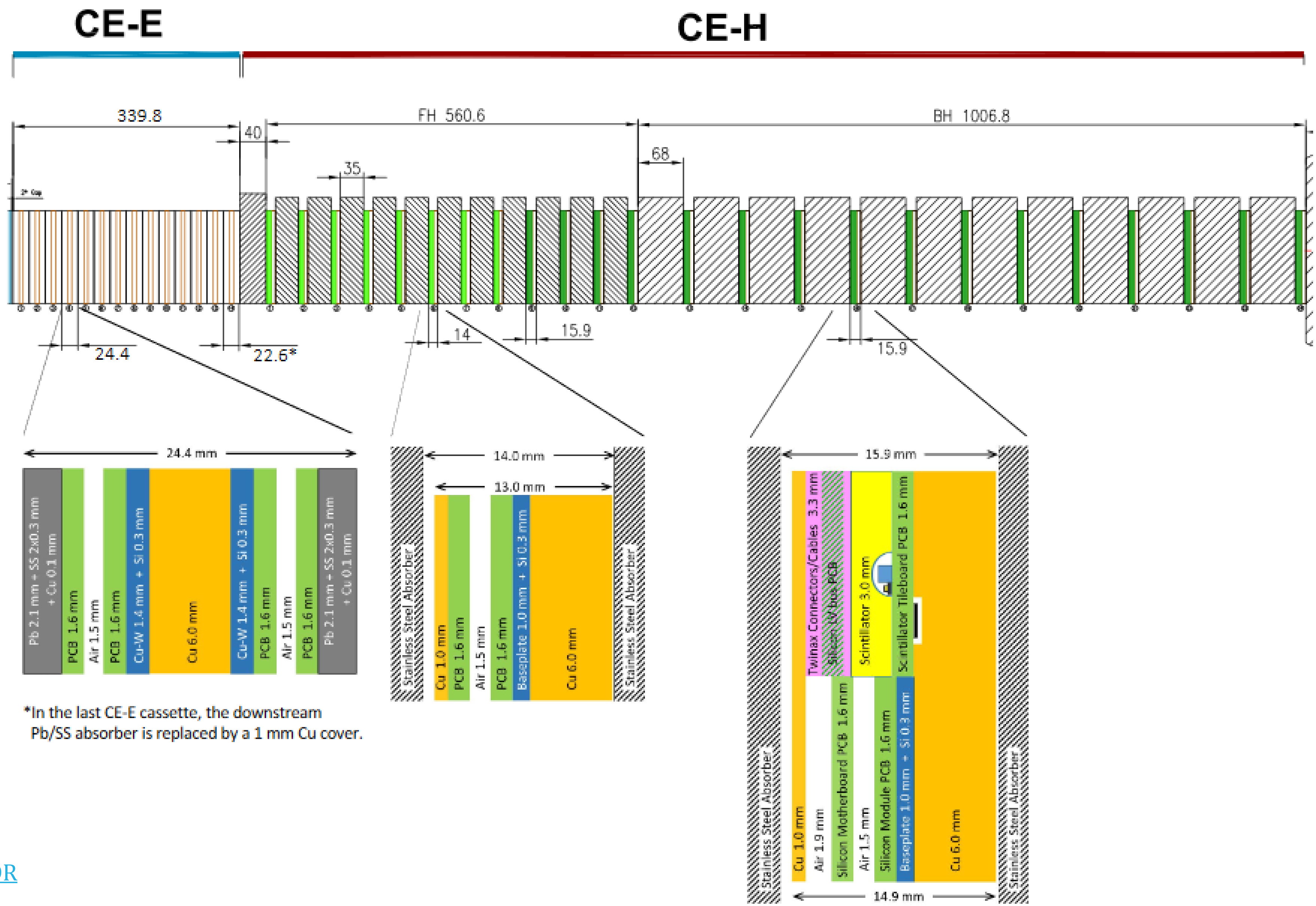

*In the last CE-E cassette, the downstream Pb/SS absorber is replaced by a 1 mm Cu cover.

CE TDR

CE structure

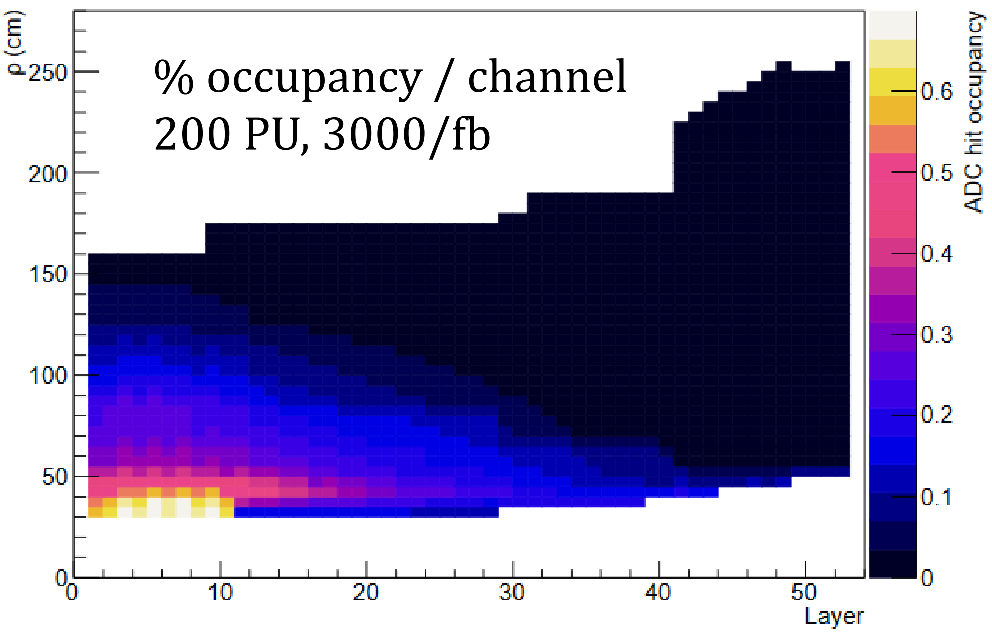

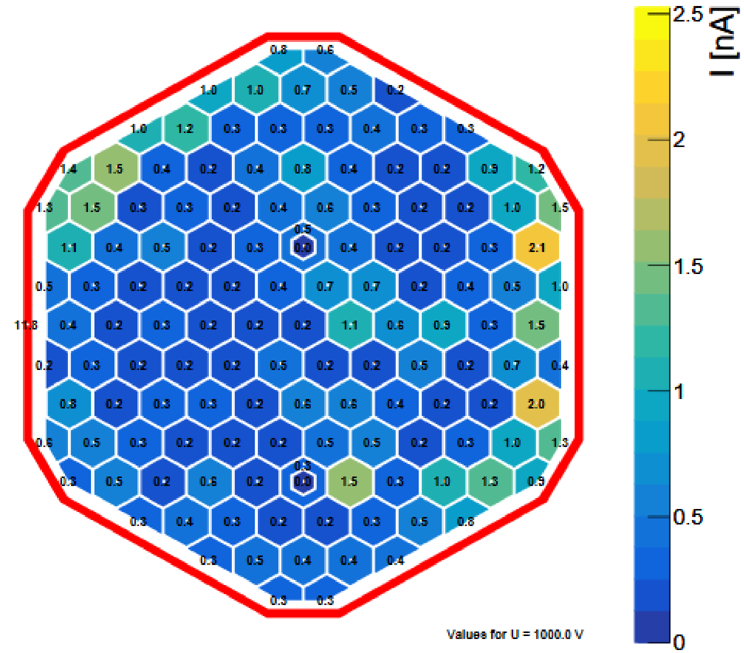

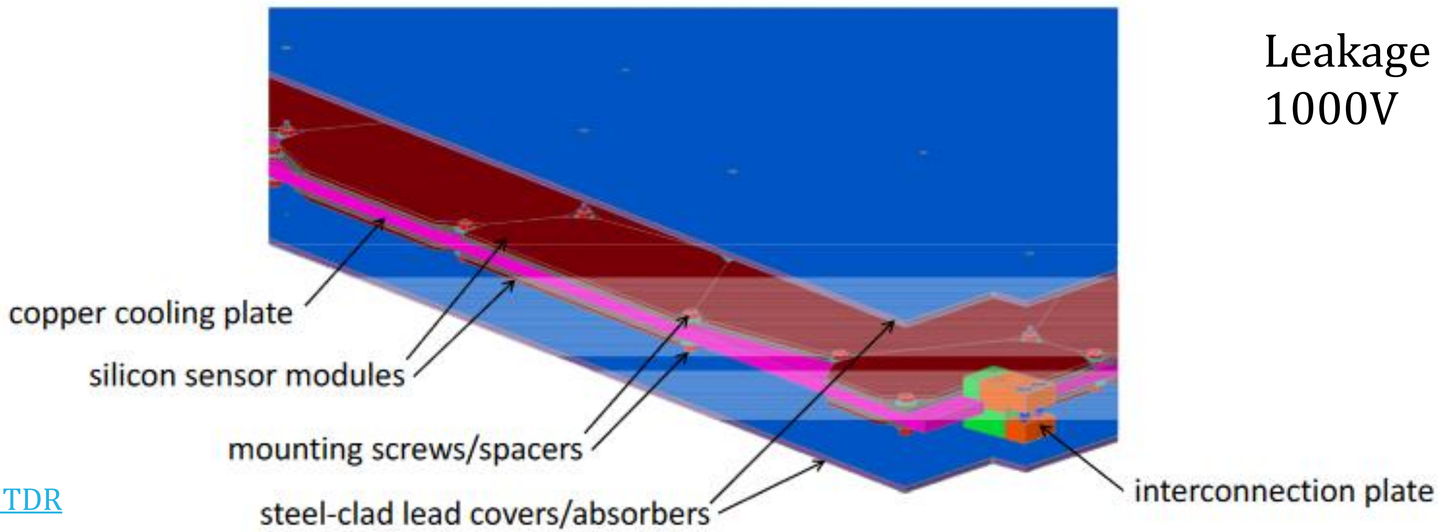

Leakage current at 1000V

CE TDR

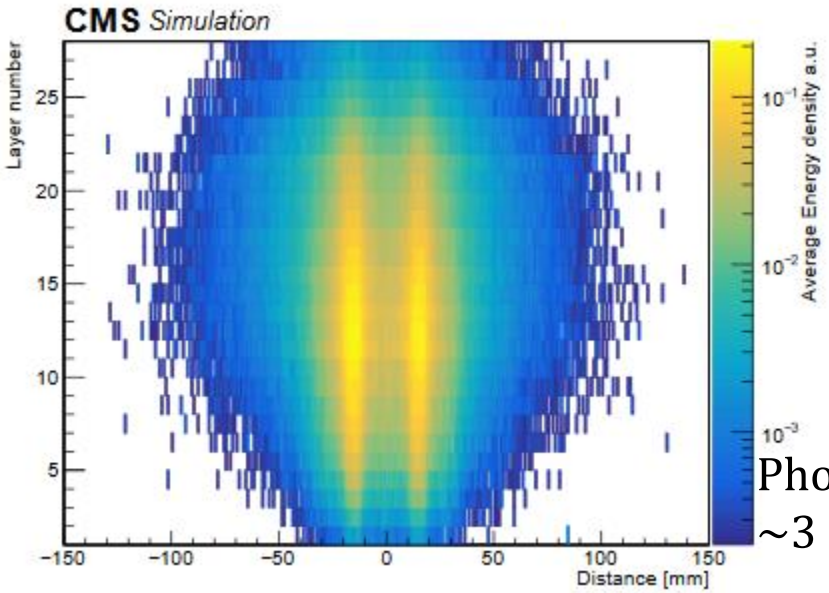

Photons separated by ~3 cm. Depth on y-axis

Photon energy resolution

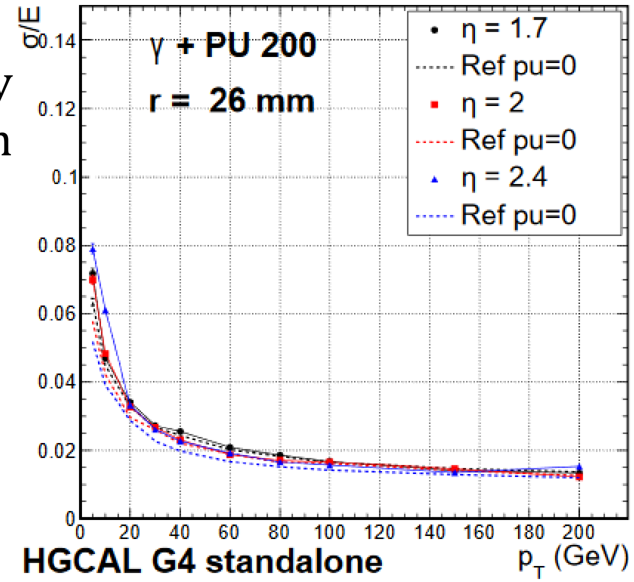

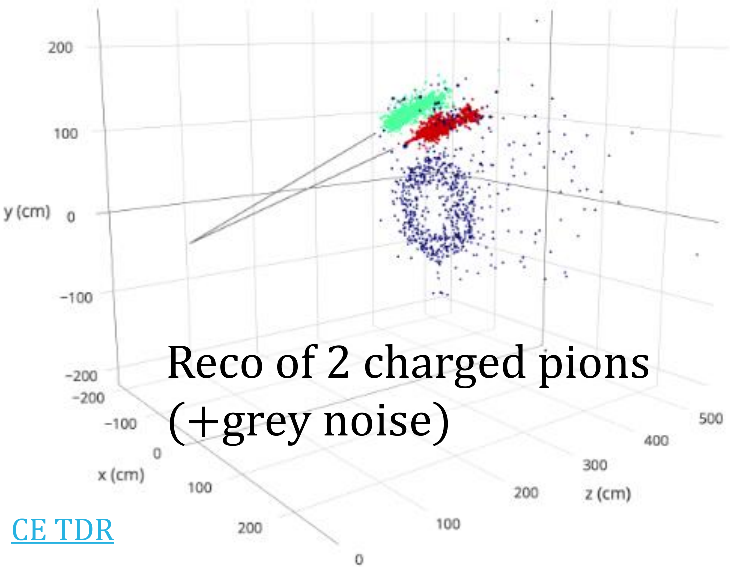

Reco of 2 charged pions (+grey noise)

Charged pion energy resolution (no tracking)

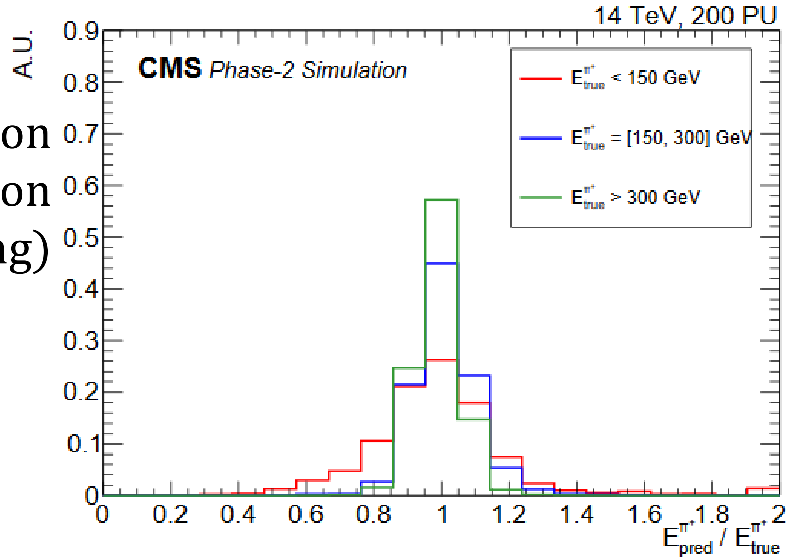

CE TDR

Muon performance

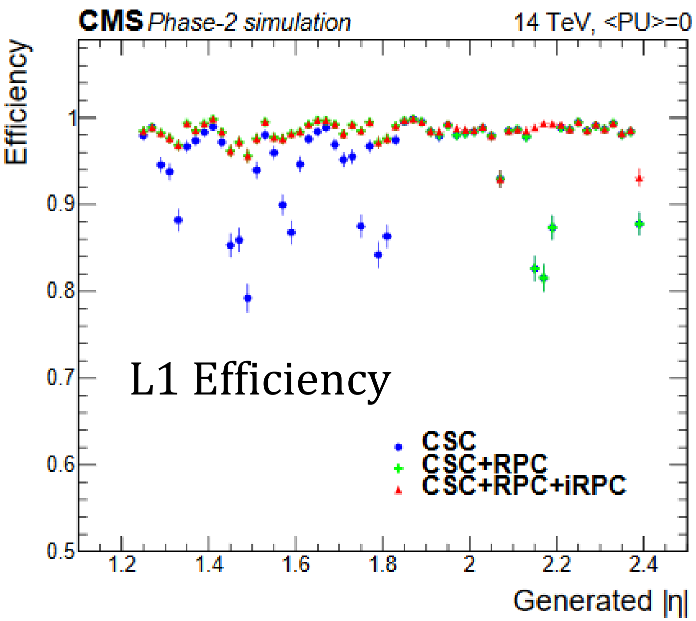

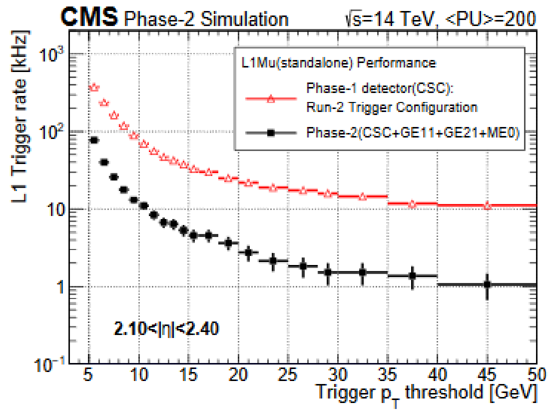

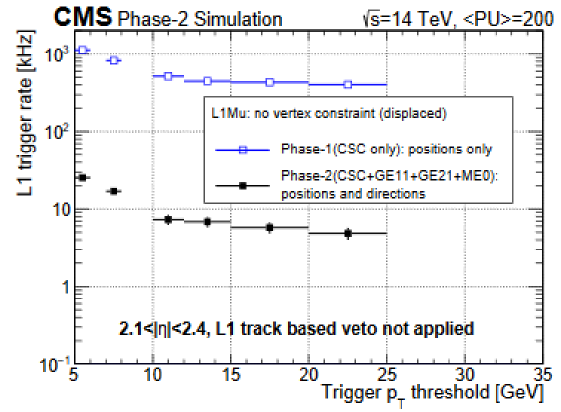

L1 rate reductions

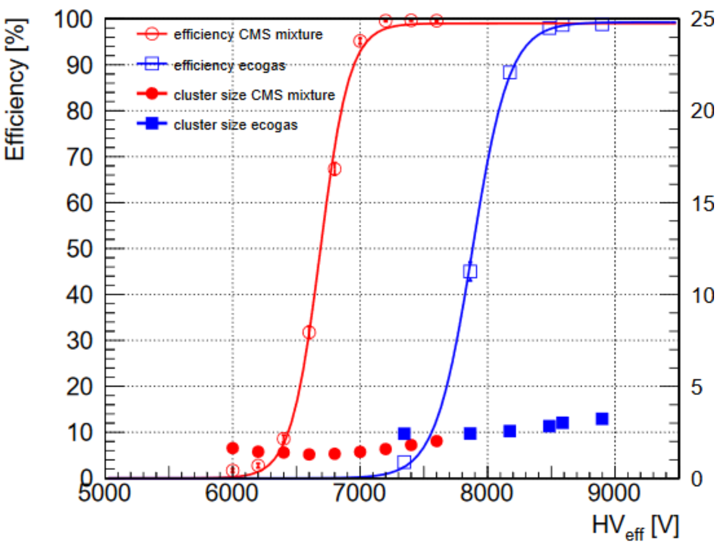

Results of tests with eco-friendly gas in RPC

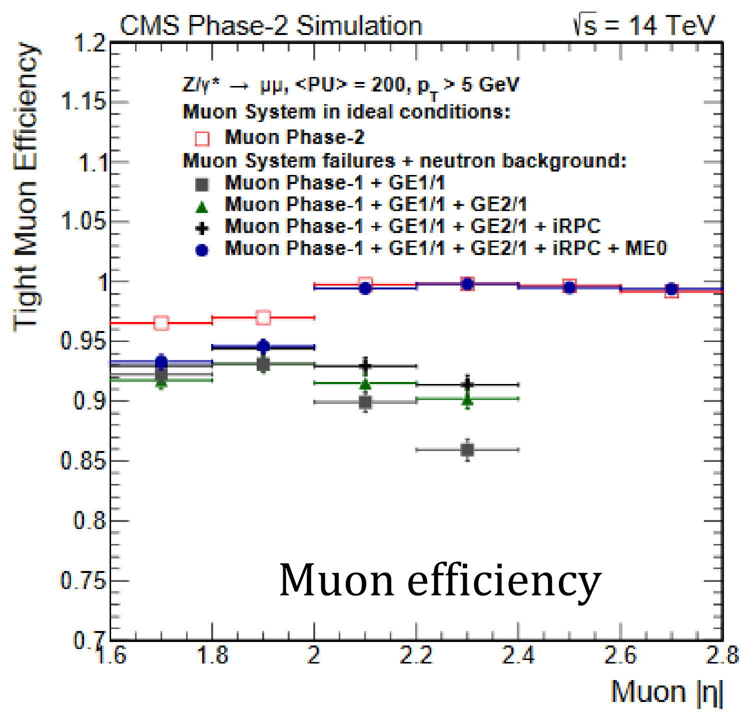

Muon TDR

Muon performance

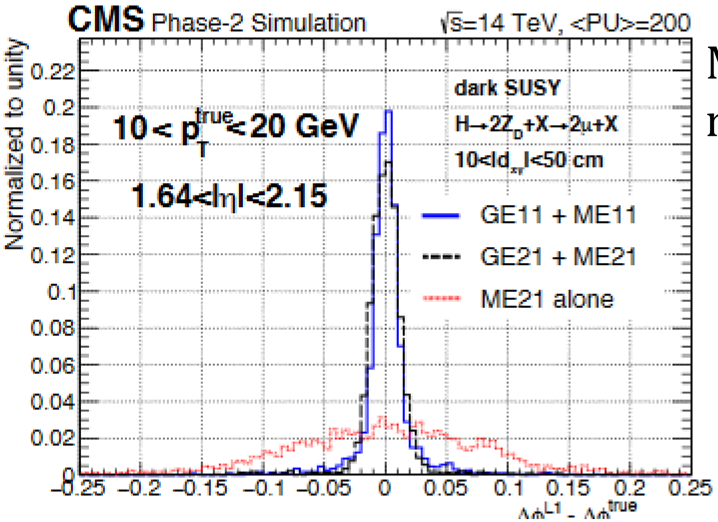

Muon direction resolution

Dphi for gen muon and pileup particles if 4 ME0 hits were found

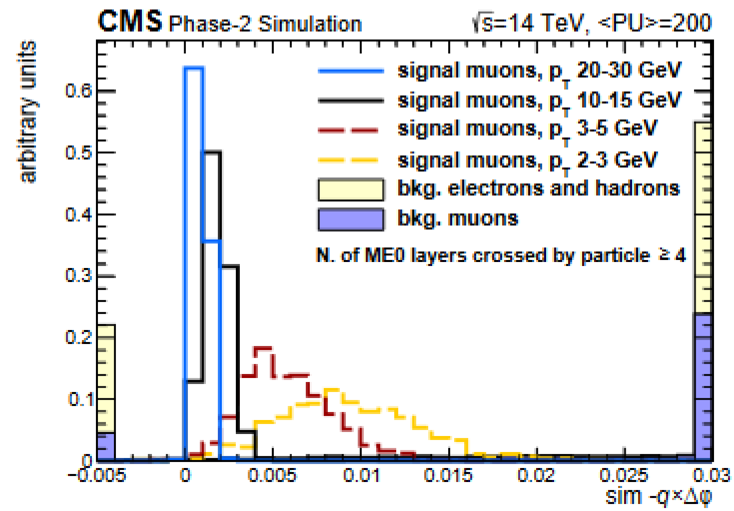

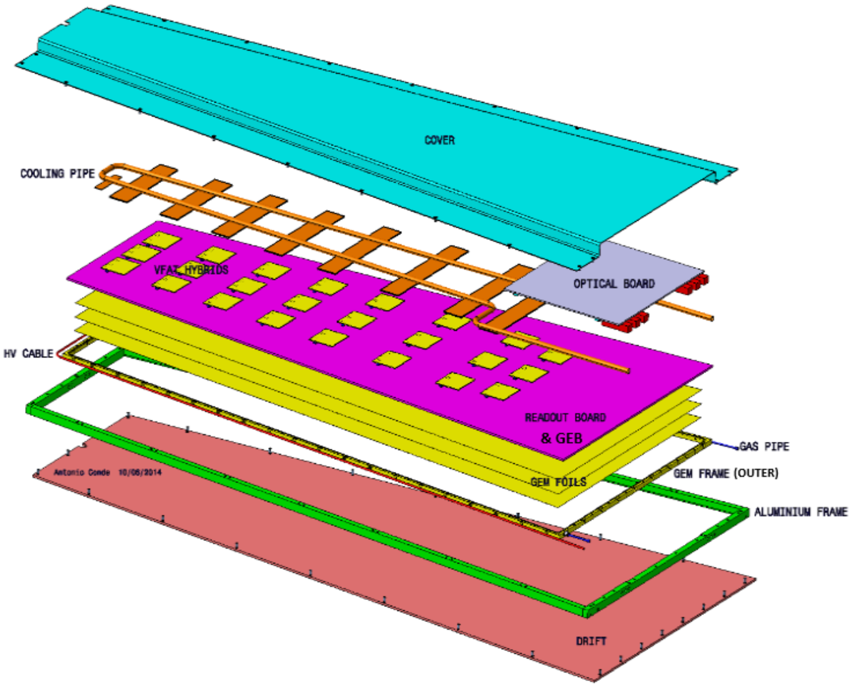

Muon TDR